Synthesis of PEG-Hydrogel Particles through Water-in-Water Emulsion for Cancer Cell Targeting

Aysu Ceren Okur

KOC UNIVERSITY
09 2015

Synthesis of PEG-Hydrogel Particles through Water-in-Water Emulsion for Cancer Cell Targeting

by

Aysu Ceren Okur

A Thesis Submitted to the
Graduate School of Sciences and Engineering
in Partial Fulfillment of the Requirements for
the Degree of

Master of Science
in
Biomedical Sciences & Engineering

Koc University
September 2015

Koc University

Graduate School of Sciences and Engineering

This is to certify that I have examined this copy of a master's thesis by

Aysu Ceren Okur

and have found that it is complete and satisfactory in all respects,
and that any and all revisions required by the final
examining committee have been made.

Committee Members:

Seda Kızılel, Ph. D. (Advisor)

Tuğba Bağcı Önder, Ph. D.

Nihan Yönet Tanyeri, Ph. D.

Date: 15 September 2015

ABSTRACT

In this study, the influence of multiple selective targeting ligands through the use of PEG hydrogel particles on targeting cancer cell surface and environment was studied. PEG based drug delivery vehicles were prepared via water-in-water emulsion technique in aqueous dextran solution. RGDS, IKVAV and cysteine–arginine–glutamic acid–lysine–alanine (CREKA) small peptides and/or combinations were conjugated to hydrogel particles as targeting ligands. Peptide conjugates were analyzed through Fourier Transform Infrared Spectroscopy (FT-IR) and X-ray Fluorescence Spectroscopy (XRF). Size and morphology of composed gel particles were characterized via Scanning Electron Microscopy (SEM). SEM micrographs showed that the sizes of synthesized particles were within the range of 16 nm-5 μm. In addition viability and uptake of PEG hydrogels by human cervical cancer cells (HeLa) was investigated using confocal microscopy *in vitro.* For particle uptake experiments, particles were loaded with Doxorubicin (Dox) and cell nucleus was fluorescently stained with 4', 6-diamidino-2-phenylindole (DAPI). Quantitative characterization of particle uptake was calculated from fluorescence intensities using ImageJ software. Cell survival experiments carried out in the presence and absence of PEG hydrogels demonstrated higher viability for the cells treated with CREKA conjugated hydrogel particles. In addition, fibrin binding assay showed that CREKA conjugated particles can bind to fibrin with 94% binding affinity compared to particles in other groups, suggesting the targeting potential of PEG hydrogel particles through CREKA functionalization. This study is promising for the development of targeted delivery vehicles, and provides the foundation of CREKA and RGDS/IKVAV mediated targeting of cancer cells.

ÖZET

Çalışmamızda, PEG hidrojel ilaç salım aracıyla çoklu ligand kullanımının hücre hedeflemesi üzerindeki etkileri araştırıldı. PEG bazlı salım araçları su içinde su emülsiyonu yöntemiyle su bazlı dextran solüsyonu içinde hazırlandı. RGDS, IKVAV ve CREKA peptidleri çeşitli kombinasyonlarla bu jel parçacıklarına eklendi. Peptitlerin varlığı FT-IR ve XRF yöntemleriyle kanıtlanırken, boyutları ve morfolojik bilgileri SEM ve DLS ile gözlemlendi. Gözlemlerimiz sonucunda sentezlenen parçacıkların boyutunun 16nm ile 5 μm arasında değiştiği saptandı. Buna ek olarak jel parçacıkları ile bekletilen hücreler için viyabilite çalışmaları ve parçacıkların hücre içine alımını görmek üzere hidrojel parçacıkları DOX ile yüklendi ve hücreler DAPI ile boyanarak confocal mikroskop çalışmaları yapıldı. Floresan yoğunlukları ImageJ ile incelenerek karşılaştırıldı. Sonuçlara göre, CREKA eklenen hidrojel parçacığının %94 oranında fibrine bağlandığı ve diğer gruplardan daha çok hücre içine girdiği gözlemlendi. Bu anlamda bu çalışma seçilimli kanser hedeflemesi için CREKA RGDS ve IKVAV'ın çoklu kullanımlarına dair bir temel niteliği taşımaktadır.

ACKNOWLEDGEMENTS

“Remember your humanity and forget the rest” As an opening to my thesis, I would like to thank all world people and scientists who would and did sign the manifesto. Without the influence of such dignified ones, neither this thesis would be written nor would I dare to involve in academia.

My special thanks to my supervisor Assoc. Prof. Dr. Seda Kızılel, for leading me such an unforgettable experience, good discussions, huge and invaluable contributions to my beloved master study. I would like to thank my committee members Assist. Prof. Dr. Tuğba Bağcı Önder and Assist. Prof. Dr. Nihan Yönet-Tanyeri for the time and knowledge that they put for valuable critics, and discussions on this thesis. I would like to thank Prof. Dr. Burak Erman, since without his presence I would not be here and learned great things that I learned from him. I would like to thank Assist. Prof. Dr. Halil Bayraktar and Assist. Prof. Dr. Ozgur Birer since their help and courses widened my perspective as well as deepened my expertise in the thesis. I would like to thank to Dr. Rıza Kızılel for his kindness and several supports for laboratory experiments. I sincerely thank to Dr. Yeliz Utku Konca, for teaching me how to teach greatly during my teaching assistantship. I would also thank to Koc University giving me the opportunity to have such a master experience in a field that I am in love.

As direct influencers, there are plenty of people I would like to thank. I would like to thank Prof. Dr. Mehmet Ali Gülgün for his influential leadership on me with all of his students, since his priority is always education, he listened my problems and never withheld his support and care like a plane tree and a “father” and made me meet the sweetest and smartest person in my life: Cleva Ow-Yang. I would like to thank Assoc. Prof. Dr. Cleva, for her fate in me, educating me at best of her and offered me the greatest opportunities. I am deeply grateful since she accepted me as a person as who I am and taught me a lot. I

want to thank the institutional founders of my university since their vision to give priority to ethics in any area.

I would like to thank my lab members for their kindness and help. Specifically, I want to thank Tugba Bal, since she was helpful and being humble despite of her huge knowledgde on what she is doing. My thanks also go to Pelin Erkoc, for her valuable contributions to this study.

Last but not least, I would like to thank my dear colleagues Dr. Barıs Yagcı and Cansu Yıldırım for their help in characterization and beautiful discussions. I am indebted to Busra Angın and Derya Cavga. Finally I owe everything more than anyone to my beloved family and friends that has been sharing this journey all the way along. My very wholehearted thanks are reserved for my family, Mustafa Karaş and, Yasemin Sevinç, Ayfer Saraç, Tuğba Somuncu, Elif Müge Baştopçu, Neslihan Sevinç, Zemre Arslan, Dilan İçar, Duygu Şükranlı and Ceren Gökçe for their unconditional love and care.

TABLE OF CONTENTS

LIST OF FIGURES

NOMENCLATURE

MW	Molecular Weight
RT	Room Temperature
PEG	Poly (ethylene glycol)
PEGDA	Poly (ethylene glycol) diacrylate
TEA	Triethanolamine
VP	1-Vinyl 2 pyrrolidone
FDA	Food and Drug Administration
NP	Nanoparticle
IONP	Iron Oxide Nanoparticles
MRI	Magnetic Resonance Imaging
UV-Vis	Ultraviolet - Visible
FT-IR	Fourier transform infrared
DLS	Dynamic Light Scattering
DOX	Doxorubicin
$\mathbf{M_0}$	Initial Amount of Doxorubicin
$\mathbf{M_f}$	Final amount of Doxorubicin

Mt	Mass of Doxorubicin at the time
Ct	Concentration at the time
Vs	Volume of subtracted sample
M∞	Mass of Doxorubicin at infinite time

Chapter 1

INTRODUCTION

Targeting of cancer cells is becoming increasingly important topic in drug delivery [1-3]. Targeting of cells through the use of specific peptides with specific affinities to transmembrane proteins can be effective strategy for tumor directed drug delivery [4-8]. For the case of targeting extracellular matrix of cancer cells, cancer targeting peptides (CTP) could be used in the design of the drug delivery vehicle. Targeting function is also useful in various other applications such as imaging[9], gene therapy[10, 11], and hyperthermia[12].

Use of peptides as targeting ligand has many advantages such as low immunogenicity, stability and ease of use. Disadvantages are related to their low affinity in targeting, and metabolic instability because of enzymatic degradation. Such disadvantages could be resolved by introducing D-type peptides as was suggested in previous studies [13].

Ligand peptides are generally selected based on their interaction of surface receptor proteins. Arginine-Glycine-Aspartic Acid (RGD) derivatives have been commonly used in peptide based targeting, where RGD is a residue in fibronectin found within extracellular matrix. RGD binds integrin receptors which is located in cell membranes and responsible for cell adhesion. Due to overexpression of several integrin receptors in tumor cells, specific targeting would be achieved. For instance, there are more than normal $\alpha_v\beta_3$ integrin receptors which mainly bind RGD as well as other receptors in integrin on most cancer cells. Another peptide that is used for cancer targeting is isoleucine-lysine-valine-alanine-valine IKVAV. IKVAV is another laminin based peptide sequence, which is located within α chain of laminin and interacts with many different cancer cell types [14-17]. It is known

as active site of laminin and is responsible for cell adhesion and tumor growth, so that it interacts with cell membrane as well. Nomizu et al. showed that both D and L forms of peptides are able to attach the cells [18]. With laminin based peptides as targeting ligands, there are also homing peptides which target extracellular matrix of the tumor area instead of cell membrane. It is important since some structures in extracellular matrix may be specific to only tumor area, and hence would provide significant information for targeting vehicle. Cysteine–arginine–glutamic acid–lysine–alanine (CREKA) is a fibrin-binding pentapeptide used as targeting peptide due to its affinity to fibrin that is found in tumor tissues but not in normal tissues [5-7].

To assess the performance of these peptides several different delivery vehicles have been used in literature. Micelles are very popular; however, their stability is limited in physiological media. Liposomes, coacervates and several inorganic nanoparticles such as superparamagnetic iron oxide nanoparticles and gold nanoparticles have been considered as are other types of delivery vehicles. Hydrogels are the most commonly used materials in tissue engineering and drug delivery. Due to controlled release properties, porous structures, designs that would respond several stimuli such as pH, mechanical and chemical, hydrogels are highly suitable materials for drug delivery. They can be covalently cross-linked, with the correct material choice, extended metabolic stability would be acquired which makes hydrogels almost excellent candidate for drug delivery applications.

Poly (ethylene glycol) based hydrogels are very popular in hydrogel applications in drug delivery, since PEG is FDA approved material, and considered as biocompatible. Due to its low surface charge, its immunogenicity is low thus PEG based vehicles can endure in blood circulation for extended periods. Dextran is another molecule that can be used for drug delivery, and tissue engineering. It is a sugar derivative, and uptake is slightly better for other biocompatible materials. The improvements in the uptake with dextran molecules

have been shown in previous studies, so that dextran based vehicles have huge potential to be easily internalized by the cancer cells[19].

In this study we developed a PEG/Dextran based hydrogel particles via water-in-water emulsion. After emulsion formation, PEG prepolymer phase was cross-linked and dextran medium was removed through successive rinsing steps. Dextran layer was found on PEG particles, which might have contributed to increased uptake. Here, we hypothesize that combination of targeting peptides such as cancer cell homing peptide and cell surface targeting peptide would significantly increase the targeting abilities and improve the uptake of drug delivery vehicles, such as PEG hydrogel particles. Functional PEG hydrogel particles incorporating CREKA and/or IKVAV and RGD were designed through water-in-water emulsion, and targeting potential of these particles was tested with HeLa cells for the first time in the literature.

In Chapter 2 of this thesis, the research on recent targeted delivery therapies and the targeting ligands have been explained. Also, developments in different type of drug delivery vehicles and applications of emulsions in hydrogels will be included in this chapter.

Chapter 3 explains materials and methods as an experimental part of the thesis. In this part, synthesis of nanoparticles via w/w emulsion technique, its gelation, and particle characterization with DLS, SEM, FT-IR have been presented. In order to show fibrin target potential of CREKA, fibrin binding assay has been included. Cell viability and uptake studies will is also presented here.

Chapter 4 discusses the results presented in Chapter 3. Chapter 5 presents our conclusion in this study and future directions have been explained.

Chapter 2

LITERATURE REVIEW

2.1 Targeted Delivery

As number of drugs increase in a therapy, side effects to human body increases. Beside side effects, adverse effects may cause serious consequences in case of combinatorial use of several drugs, as in chemotherapies. Even without adverse effects, drugs may show side effects due to low selectivity, which is another goal for targeting to inhibit. With targeting ligands, chance of directing each drug to their original target would increase rather than an ordinary binding because of low energy. Same principle is also used in gene delivery for the treatment of various diseases. Moreover, in MRI technique, the delivery of imaging agents towards tumors tissue rather than healthy cells would improve signal quality greatly, increasing the diagnosis accuracy. Finally, the hyperthermia is another technique for cancer therapies, where agents dissipate heat in order to kill the cancer cells. It is critically important to localize hyperthermia agents in tumor rather than healthy cells; otherwise its effects would be detrimental.

2.1.1 Targeted Delivery Therapies

2.1.1.1 Hyperthermia

Magnetic Fluid Hyperthermia (MFH) is one of the techniques that have been used for cancer therapy. This therapy consists of exposure of alternating magnetic field to the delivered substance thus, releasing heat so that tumor would be destroyed with delivered energy. The main function of the hyperthermia agent is to absorb the energy and convert it to a cytotoxic amount of heat, since it is found that tumor cells are more prone to heat then

healthy cells, this technique as a cancer therapy has a potential. First hyperthermia experiments with magnetic materials were done by Gilchrist et al. in 1957. First clinical trials were carried out by Jordan et al. proving that treatment was successful for several tumors[20]. Specifically, the regional hyperthermia treatment was used clinically as a first trial on prostate cancer by Johannsen [21] on 2005. Lately Gordon et al, used microparticles of yttrium doped iron oxide for MRI combined hyperthermia treatments of liver cancer [22]. However hyperthermia has its pros and cons. It is generally preferred as local treatment instead of regional or a complete treatment of body. Also the treatment can be applied between 42-45°C for local hyperthermia [23, 24]. Therefore it is very important that, temperature affects only the targeted site but not healthy cells around.

To achieve cancer targeting for hyperthermia several targeting ligands that are FDA approved since today can be used [25]. In addition, peptide based ligands can also be used for targeting of cancer cells. Sadhuka *et al* showed EGFR –α membrane receptor which is overexpressed in cancer cells) can be targeted by a peptide based ligand for hyperthermia therapy [26]. Another study by Shah *et al.* presents a hyperthermia agent consists of magnetic core with chemotherapeutic effect peptide called mitochondria-targeting pro-apoptotic amphipathic tail-anchoring peptide (ATAP) with utilization of RGD derivative helping internalization for cancer cell uptake on malignant brain and metastatic breast cancer cells [27]. In their study, the authors showed that such targeting would significantly increase the uptake and efficacy of the treatment. However, for magnetic particles peptide based targeting may have failures, since such particles would be heavy and peptide selectivity may not be enough for such applications.

2.1.1.2 Gene Delivery

Gene delivery or gene therapy essentially involves transferring genes into the body for therapeutic aims [28]. Gene therapy is mainly used for diseases caused by genetic disorder especially for several immune system diseases; e.g. Chronic Granulomatus Disorder, Severe Combined Immune Deficiency and neurodegenerative diseases such as Parkinson disease and Huntington disease. Gene delivery is also used in various cancer therapies. The delivered gene is used for replacing or silencing the defective gene that causes the disease[29].

An important limitation in gene therapy is the delivery of gene to the related tissue or cell as well as observing the response. The problem is mainly because of viral vector use for transfection of genes. Due to several problems related to viral vector use, such as mutations during insertion, immunologic response of body and vector size limitation for carrying enough genes, non-viral systems are needed [30].

Rather than using viral vectors, targeting agents would be benefited in such therapies. There are several upregulated receptors in diseased organisms that would be utilized for the purpose. Hyper activated protein kinase Cα (PKCα) for tumor cells[31], CD34 that is abundant for human hematopoietic stem cells[32] and transferrin receptor antibody for brain delivery[33] are few of them[34].

2.1.1.3 Imaging

MRI drugs have been expected to improve image contrast between normal and diseased tissue to recognize healthy or pathological tissues, and most of different contrast agents have been suggested for this purpose. Up until now, paramagnetic contrast agents have been used in MRI studies such as paramagnetic gadolinium chelates [35]. These agents work through shortening the T_1 relaxation time (longitudinal relaxation time) of water in tissues, whereas, superparamagnetic nanoparticles have diagnostic sensitivity and

specificity due to their superior properties like higher molar relaxivities, and ability to shorten both T_1 relaxation time and T_2 transversal relaxation time. Their effectiveness depends on their size, charge and coating properties, but can be increased through further modification of the surface with biologically active substances like antibodies, receptor ligands, polysaccharides, proteins, etc. [36].

Targeting of cancer cells with MRI has several examples in literature. For instance, S. Boutry et al. targeted endothelial inflammatory adhesion molecule E-selectin with a superparamagnetic MRI contrast agent coated with dextran [37]. Contrast agent was further functionalized with the addition of a synthetic mimetic of sialyl Lewisx, a natural ligand of E-selectin expressed in leukocytes. Both *in vitro* (on cultured human umbilical vein endothelial cells) and *in vivo* (on a mouse model of hepatitis) results proved that this new contrast agent recognized endothelial E-selectin. Therefore it was considered as appropriate for diagnosis of inflammation with MRI [37]. Another study by Serres *et al.* showed increased contrasting capability in MRI using iron oxide particles conjugated with antibody. Upregulation of VCAM-1 on metastatic lesion of brains was verified by the same group, where the researchers designed an agent conjugated to anti-VCAM, specific for metastatic cells. Hence, uptake of anti-VCAM by metastatic cells was not shown, creating an enhanced contrast and allowing a technology to detect metastatic cells in early forms [38].

2.1.1.4 Drug Delivery

Bare use of drugs in metabolic systems results in severe antagonistic effects for complicated conditions as in case of cancer and some pathogens[39]. In addition to localization at the diseased site, drug molecules also interact with each other resulting in increased or diminished efficiency on therapeutic effect[40]. Moreover, without targeting strategy, these molecules would also interact with untargeted and healthy sites and cause severe side and adverse effects. In order to minimize these unwanted interactions, drug

molecules' tendency for interaction should be prevented until drug reaches its target. This could be achieved through coating, encapsulating and conjugating the drugs by other molecules, such as targeting vehicles as nanoparticles or polymeric coatings[41].

2.1.1.4.1 Drug Delivery Vehicles

2.1.1.4.1.1 Inorganic Nanoparticles

Nanoparticle based drug delivery is an attractive field due to several advantages such as small size and various physical properties of nanoparticles[42]. Use of nanoparticles for biomedical studies ranges from 10 nm to several microns[43]. Due to their size, NP's can easily diffuse into peripheral tissue in case of cancer by exploiting the enhanced permeation and retention (EPR) effect, which can mostly be observed in diseased endothelial tissue[44].

Moreover, nanoparticles can be loaded with drugs through different routes, such as encapsulation, surface attachment and entrapment[45]. Another benefit of nanoparticle use is the reduction of multidrug resistance (MDR) for most hydrophobic drugs, which is a large portion of general drugs. MDR is caused by ATP binding cassette (ABC) which is an overexpressed transporter in cancer cells. ABC causes MDR by pumping the most hydrophobic drugs out of the cancer cells. To overcome MDR, SPION's are used with DOX conjugation as an example. Researches showed that DOX with SPION conjugation could overcome MDR, so that effective delivery of the drug could be achieved [46].

Active targeting includes the functionalization of the nanoparticle by several targeting agents. This usually would be a multistep process including coating and targeting molecules adhesion to the structure and loading the drugs via several ways, such as covalent conjugation or physical adsorption [44]. As a result there are several vehicles that are designed including, nanotubes, quantum dots, polymersomes and dendrimers[47].

2.1.1.4.1.2 Micelles

Polymeric micelles have been commonly used for drug delivery purposes. Such micelles are nanoscale (10-100 nm) self-assembled colloid particles that consist of amphiphilic block or graft polymers in aqueous media [48]. The hydrophobic core of micelles enable encapsulation of hydrophobic drugs [49]. Micelles have been used in several studies for drug delivery despite their issues as stability in blood circulation and drug loading efficiency [5, 50-52]. In order to form micelles, critical micelle concentration (CMC) needs to be measured. Due to easy fabrication of micelles, it can be a promising platform for drug delivery, provided that various concerns are resolved [53].

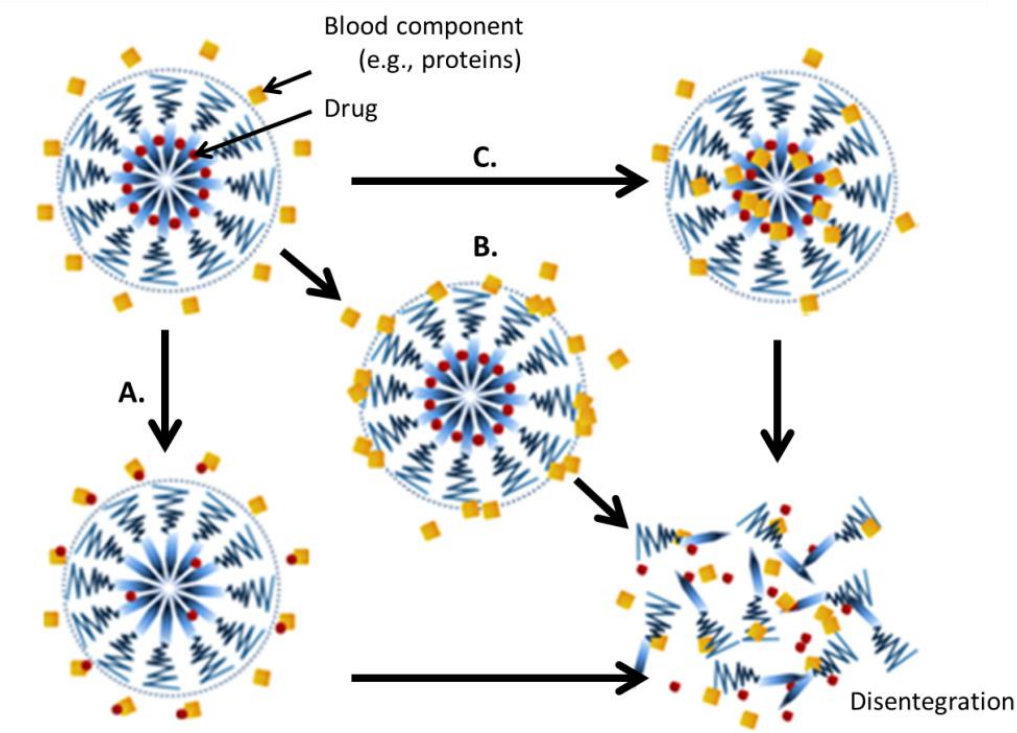

Figure 1. Mechanisms of micelle disintegration in the presence of serum proteins. A. Drug extraction. B. Protein adsorption. C. Protein penetration

2.1.1.4.1.3 Liposomes

Liposomes consist of aqueous core surrounded by lipid bilayers. Lipids can be either natural or synthetic. Phospholipids are natural lipids that are biocompatible and have love immunogenicity. Their main advantage is the capability to keep several drugs with altered lipophilicities. Aqueous drugs would be carried in aqueous core whereas, the high lipophilic cores can be carried within lipid bilayer [54].

Liposomes range in size between 50 nm to 5 μm. Unilamelar liposomes which have one lipid bilayer that mainly carries hydrophilic drugs in its aqueous core have diameters of 50-250 nm, whereas the multilamellar ones that have multiple lipid sections which allow them to carry lipid-soluble drugs up to 5 μm [55].

Tumor targeting can also be achieved by liposomal therapies. Even though liposomes have issues on overcoming phagocytic clearance in lymphatic system, it shows growing potential in drug delivery studies. In general vector targeting has been achieved through such systems. Liposomes can also self-assemble, and their stability may raise various concerns [56].

2.1.1.4.1.4 Hydrogels

Hydrogels have polymeric network structure that contain large amount of water within their pores. The network consists of cross-linked polymers via covalent bonds, hydrogen bonds, electrostatic interactions or physical entanglements [57]. Hydrogels are mainly known with their absorption of water, since they can absorb several hundred times of their weight of water due to hydrophilic properties of polymers such as PEG [58], PVA [59] and PAA [60]. Hydrogel studies started with poly methacrylate derivative hydrogel structures that are produced in 1960s [61-63]. PAA was used as super adsorbent for water, whereas, PVA and PEG were used for biomedical applications. Because of soft nature of hydrogels that is similar to tissue mechanical properties, hydrogels were commonly considered as

biocompatible platforms for cell studies. With such synthetic polymers, natural polymers such as alginate, collagen, fibrin, gelatin, dextran and hyaluronic acid have been also used in hydrogels.

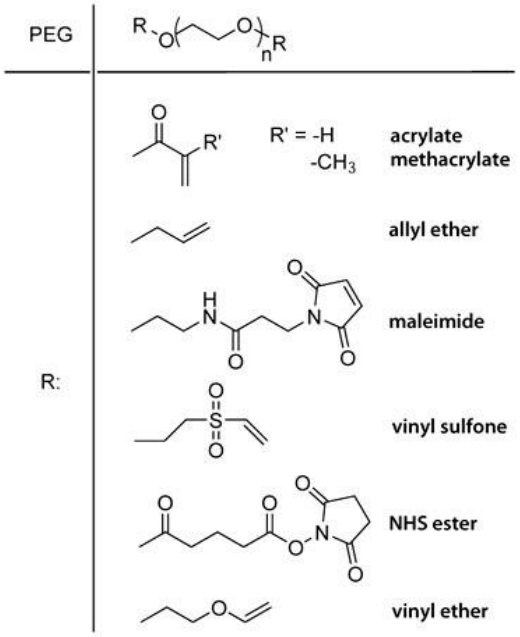

Figure 2. Active end groups for PEG crosslink

2.1.1.4.1.4.1 PEG Hydrogels

PEG is FDA approved synthetic polymer that has been extensively used in biomedical studies. PEG does not elicit immune response and has been considered as biocompatible. Due to low surface energy of PEG, non-specific interactions with the structure and proteins would be diminished. PEG can be crosslinked through various strategies. For example, to crosslink PEG diacrylate, PEG is attached to several reactive groups that are activated via ionizing radiation as is shown in Figure 2. These end groups would be initiated with

radicals generated with light; Irgacure (635 nm), and Eosin Y (514nm) and chemical radical generation. In chemical radical reaction several reactive groups, which would affect toxicity. PEG can also be crosslinked through free radical photopolymerization. Photoinitiator eosin Y has been commonly used with triethanolamine, where covalent crosslinking can be achieved through visible green light as chain growth polymerization.

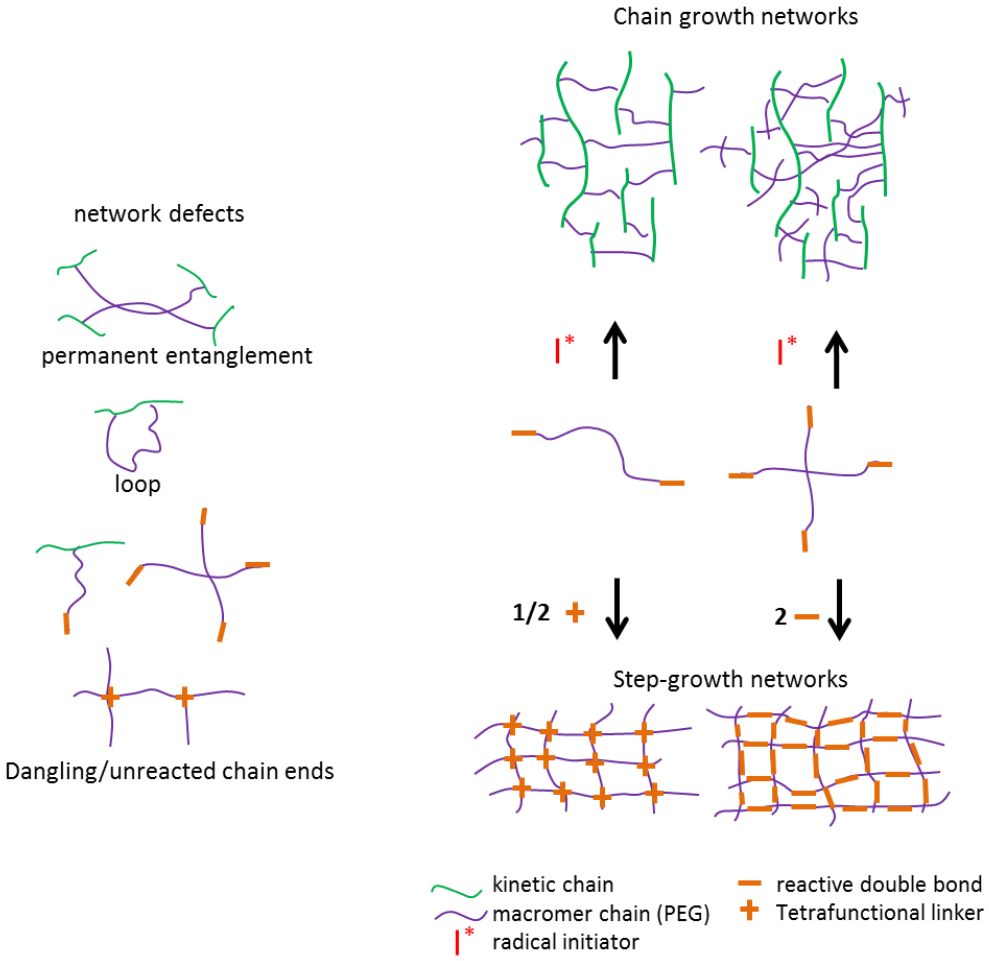

Figure 3. Branching and crosslinking mechanism during polymerization

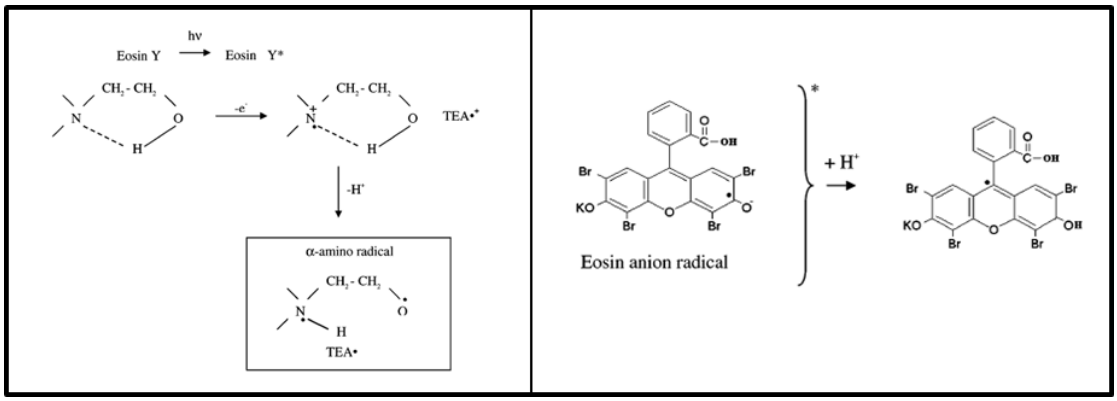

Figure 4. Eosin Y & TEA Initiation in PEG Polymerization[64]

In this thesis, PEG hydrogel particles were obtained through free radical photopolymerization of PEG, and hence eosin Y and triethanolamine (TEA) was used with acrylate ended bifunctional PEG monomer. Reaction mechanism starts with excitation of eosin Y as initiator to its triplet state via green laser light (514 nm). In this state electron is transferred from TEA to Eosin Y, producing α-amino radical TEA (TEA*) and TEA* starts free radical polymerization. With the accelerator molecule 1-vinyl 2-pyrrolidone (VP), PEGDA is cross-linked and with excessive crosslinking gel formation occurs (Figure 4).

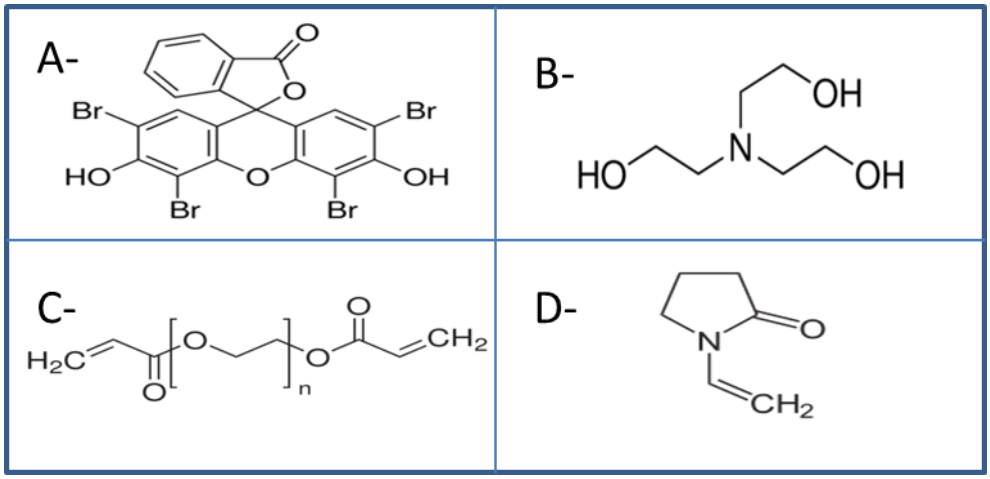

Figure 5. Chemical structure of polymerization agents. A- Eosin Y, B- Triethanolamine, C- PEG-DA, D- 1-Vinyl 2-Pyrrolidone

2.1.1.4.1 Targeting peptide molecules

Selective targeting of species requires specific targeting molecules to distinguish the target region than other parts of the body. Targets would be specific surface proteins of cells, extracellular matrix elements or any molecule that would differ from healthy body parts. In general, there are several signals for diseased cells or tissues. Their microenvironment would be different; their extracellular matrix composition may change due to change in cell behaviors or cells itself. For instance cancer cells mostly express higher number of several surface proteins in order to increase angiogenesis and attaching strongly to their environment. To target these regions, rather than inorganic targeting molecules, mimicry of biological molecules were utilized. Peptides were designed and have been used to target such overexpressed surface proteins and receptors as well as extracellular matrix. In this section, some of the peptides in the literature and those that were used in this study will be briefly discussed.

2.1.1.4.1.1 RGDS

RGDS is a four amino acid peptide sequence which was found to be responsible from cell adhesion as a part of fibronectin [65]. It is the adhesion site of many structures found in extracellular matrix which can be recognized at least 20 known integrins that is responsible from adhesion. While RGD remains invariant, serine is shown to vary for different structures [66]. Despite its small size, its activity is quite specific with adhesion sites of cell surface receptors, mainly integrins.

Integrins are overexpressed in many cancer cell lines, since these receptors take part also in angiogenesis, which is crucial for tumor growth [67]. As carcinoma, HeLa cells overexpress $\alpha_v\beta_3$ and $\alpha_v\beta_5$ integrins which would be used as targeting site by RGDS peptide [68]. The RGDS involvement as a targeting ligand into delivery systems is shown in literature to be increasing the targeting efficiency tremendously [69, 70]. Breast [71] and prostate cancer [72, 73] and pancreatic carcinoma [74] treatments have also been studied with RGDS showing the targeting potential of systems with RGDS [75].

2.1.1.4.1.2 IKVAV

IKVAV is a laminin derived, five amino acid peptide sequence that is presented as responsible from angiogenesis and tumor growth [14]. IKVAV binds 110 kDa laminin 1 receptor, known as nucleolin as shuttling protein found on different cancer types [76, 77]. For instance, nucleolin has been showed on HeLa cell surfaces [77] with excellent ability of targeting PEG conjugated DNA parts. IKVAV can also bind $\alpha_3\beta_1$ and $\alpha_3\beta_1$ integrins, which are found and overexpressed in some type of cancer cell lines such as breast and prostate [16, 78]. Thus, such cell surface receptors would be used for targeting several cancer types by using IKVAV sequence as targeting ligand for drug delivery purposes.

2.1.1.4.1.3 CREKA

CREKA is a tumor homing pentapeptide, which targets fibrin deposition found in epithelial tumor tissue environment [5, 7]. It targets, collagen IV α_2 chain that is found in fibrin/ fibrinogen structure [79]. Normal epithelial cell extracellular matrix includes collagen IV [17]. However, in atypical tumor extracellular matrix, amount of collagen 4 is elevated. This difference allows CREKA to be used as targeting ligand for tumor environment. Several studies have shown both *in vivo* and *in vitro* studies proofing the homing ability of CREKA for various cancer types [5, 6]. CREKA preservation of its targeting ability in conjugated form from cysteine group has also been shown in literature [5]. Both *in vivo* and *in vitro* studies demonstrated promising targeting results with CREKA conjugated delivery platforms [80].

2.1.2 Emulsion

In this thesis, to synthesize PEG hydrogel particles, emulsification strategy on hydrogel particles was utilized. Emulsions are metastable colloids that consist of two phases; one dispersed in other. In principle, emulsion systems can be formed with two immiscible phased that have non-zero surface tension. Direct emulsions consist of oil phase in water phase, whereas inverse emulsion has water phase in oil phase. The phase that droplets are formed called as “dispersed phase”. The medium that includes dispersed particles are called as “continuous phase”. Sometimes, there may be multiple phases one in another, or there may be continuous phase droplets in dispersed phase droplets. These emulsion systems are known as double emulsions. Due to density differences, viscoelastic behaviors of emulsions would differ from each other.

The emulsions can be destroyed either through Ostwald ripening or coalescence mechanism. Ostwald ripening occurs due to diffusion of dispersed phase through continuous phase. In case of coalescence, there is a hole formed in the film, causing the formation of larger droplets in continuous system as a result of fusion of two droplets. To

prevent such destruction, surface active species, surfactants, that would locate surface between two phases would be needed and definitely increase the stability of these systems [81].

The emulsions are preferred for lipophilic drug loading purposes due to their two phase system, e.g. oil in water and as inverse emulsion, water in oil. For instance, rapamycin, a water insoluble drug, which is used for antibiotics and a potent anti-tumor agent, was studied with nanoemulsion as drug delivery vehicle. In such system, PEG and propylene glycol were used as phases with surfactant called as Triacetin. In this study, it was also stated that nanoemulsions showed higher stability than microemulsions as a result of polydispersity index measurements up to 12 months, due to ultralow interfacial tension of nanoemulsions thus showing higher potential as drug delivery system [82].

Beyond anti-tumor drugs, nanoemulsion system would also be beneficial for gene delivery. Nanogels that were synthesized through microemulsion techniques were also investigated for gene delivery studies. As an example, McAllister *et al.* produced polymeric nanogels with inverse microemulsion technique [83]. These gels had sizes up to 200 nm and were based on PEG, where they were used as a vector to deliver DNA. The gels demonstrated high level of uptake by HeLa cells through rhodamine B labeling. Their high uptake suggested the potential of nanogels for drug and gene delivery.

Chapter 3

MATERIALS & METHODS

3.1 Materials

Potassium Chloride (KCl), Sodium Bicarbonate ($NaHCO_3$), Potassium dihydrogen phosphate (KH_2PO_4), Fluorescein Acrylate, Eosin-Y (EY) (91%), 1-vinyl- 2-pyrrolidone (VP), Dextran 60 kDa, Poly(ethylene glycol)diacrylate (PEG DA, molecular weight: 575Da), Triton X-100 were purchased from Sigma. Triethanol-amine (TEA) (99.5%) and 37% formaldehyde were obtained from Merck. Phosphate Buffer Saline (PBS) was purchased Gibco (CA). Hydrochloric acid (HCl) and Sodium Hydroxide (NaOH) were purchased from Riedel-de Haen. Amicon Ultra Centrifugal Filter (NMWL: 10000) was obtained from Merck Millipore. Doxorubicin Hydrochloride was purchased from MP Biomedicals (Solon, OH). DAPI (4', 6-Diamidino-2-Phenylindole, Dihydrochloride) was purchased from Invitrogen Co (Carlsbad, CA). Short peptide arginine-glycine-aspartic acid- serine (RGDS) (MW: 433 Da), isoleucine-lysine-valine-alanine-valine (IKVAV) (MW: 528 Da), cysteine–arginine–glutamic acid–lysine–alanine (CREKA) (MW: 605 Da) was purchased Elim Biopharmaceuticals. Acrylate PEG *N*-Hydroxysuccinimide (Acryl-PEG-NHS, MW: 3.4 kDa)was purchased from Laysan Bio. Dialysis cassette (MW cutoff: 3.5kDa) was obtained from Pierce. 0.2μm and 0.45 μm Cellulose and Nylon Filters were purchased from Merck. Petri Dishes were purchased from Nunc. Dulbecco's Modified Eagle Medium (liquid, with 4.5g/L D-glucose and sodium pyruvate) (DMEM), L-Glutamine, was purchased from Invitrogen. Fetal Bovine Serum (FBS) was obtained by Bioindustries. Penicilin/streptomycin was purchased from Gibco. Trypsin – EDTA was obtained from Genlantis. Fibrin *In Vitro* Angiogenesis Assay was obtained from Merck Millipore. Cell-Titer-GLO Luminescent Viability Assay Kit was obtained from Promega.

96-well cell culture plate and 6-well, 24-well plate cell culture plates were purchased from Greiner Bio-One. Microscopy slide was purchased from Fisher Scientific. Cover slide was obtained from Isolab.

3.1.1 Methods

3.1.2 Emulsion Preparation & Gel Formation

1g Dextran is solved in a buffer containing 0.22 M KCl, 10 mM Na_2HPO_4 dibasic. To functionalize PEG nanogels CREKA, RGDS and IKVAV peptides were used. CREKA was directly bound to PEG acrylate groups in PEGDA via thiol ether linkage group with sulfur on cysteine. RGDS and IKVAV were conjugated PEG particles within Acr-PEG-Peptide structure. Acr-PEG-IKVAV and Acr-PEG-RGDS conjugates were obtained with conjugate reaction of peptides to Acr-PEG-SVA from SVA group. 1 mg/ml of RGDS/IKVAV and 10mg/ml of Acr-PEG-SVA were separately prepared in 50 mM $NaHCO_3$ at pH 8.2. Acr-PEG-SVA solution was mixed with peptide solution in dropwise with molar ratio of 1:1. The conjugation reaction was carried out for 2 h in room temperature and dialyzed with distilled 18 mQ water to remove unreacted species. The synthesized Acr-PEG-RGDS and Acr-PEG-IKVAV conjugate structure was confirmed with Fourier Transform- Infrared Spectroscopy (FT-IR) (Thermo Scientific, Nicolet iS10 FT-IR spectrometer).

Prepolymer solution was prepared with 500 mM PEGDA (MW:575 Da), 37.5 mM TEA (Coinitiator) and 6.3 mM VP (accelerator) and 0.025 mM Eosin Y (Initiator) was used. The pH of prepolymer solution was adjusted to 8. For gel conditions containing different combinations of peptide include 0.5 mM CREKA, 2.4 mM RGDS and IKVAV peptide or peptide conjugates. Before mixing dextran and PEG prepolymer solutions, both are sonicated via ultrasonication for 1min. Prepolymer solution was added to dextran solution dropwise. Mixture was stirred via magnetic stir bar with 1250 rpm for 45 minutes. After emulsion formation mixture was exposed to green light (λ: 514 nm, P: 2.5 mW/cm^2) using

Argon ion laser (Coherent, Innova 70C) within 65 seconds in 3 ml petri dishes. Laser exposed gels were rinsed with 10000 pore sized centrifugal filters (Millipore, Merck). Before storage at +4 °C, gels were frieze dried (Labconco, FreeZone 2.5 liter Benchtop Frieze Dry System).

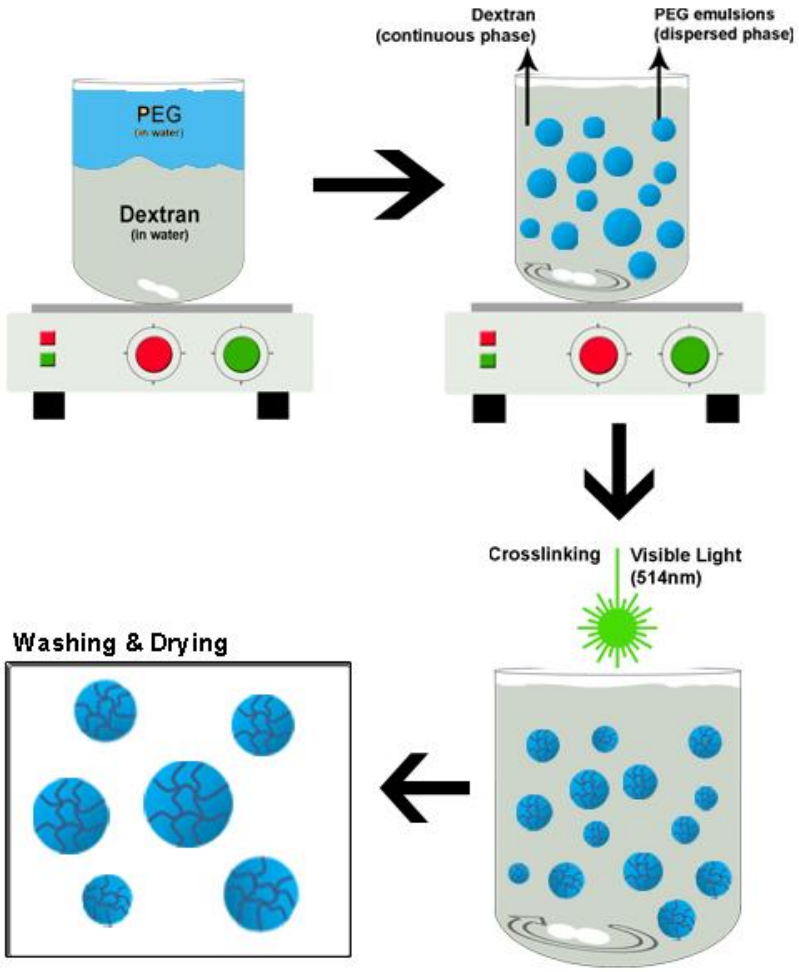

Figure 6. Schematics of PEG Hydrogel Synthesis via Microemulsion Method

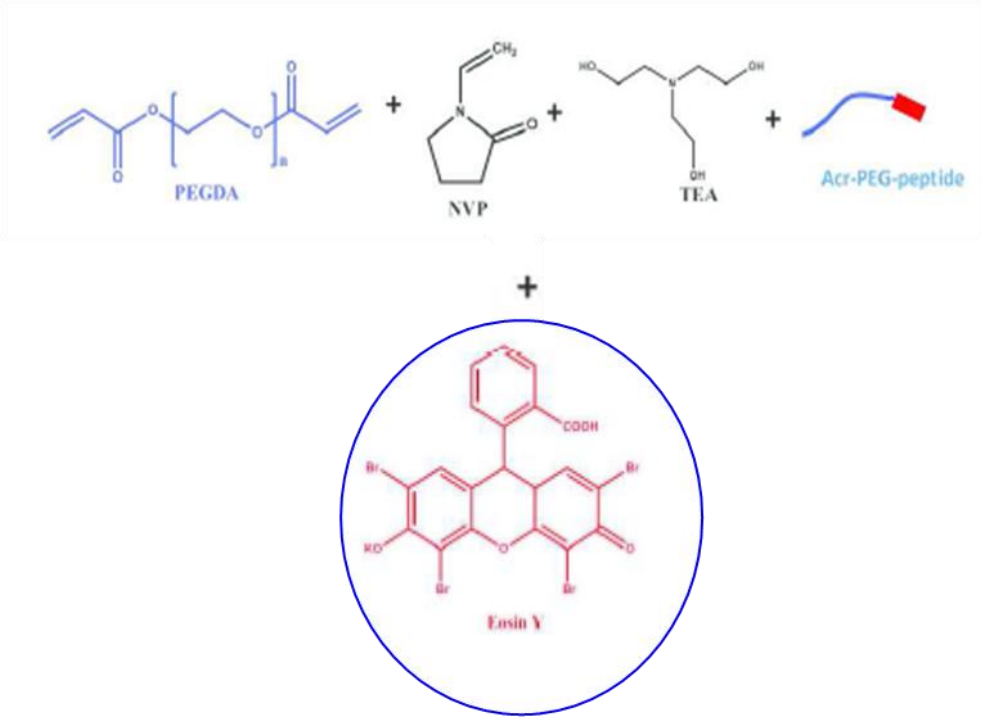

Figure 7. Prepolymer species

3.1.3 Characterization

3.1.3.1 FE-SEM

Field Emission Scanning Electron Microscope (FESEM) images were used to confirm particle formation and determine the size distribution of hydrogel particles. The microscope that is used in this study is Zeiss Ultra Plus FESEM at an acceleration potential of 1kV. All samples were frieze dried and placed on a carbon tape on aluminum stubs in powder form. Then each sample surfaces were 3 nm gold coated using Cressington Sputter(108 Auto with Cressington Thick Monitor MTM-10)

3.1.3.2 FT-IR

FT-IR spectra are used to confirm incorporation of peptides to the hydrogel particles by using Thermo Scientific iS10 FT-IR, with range 650-4000 cm^{-1} and single reflection diamond ATR. Samples were prepared in both powder and bulk gel form.

3.1.3.3 Raman

Raman Spectra is used to confirm IKVAV incorporation to the hydrogel particles by using Renishaw Invia, Raman Microscope. Samples were prepared in powder form.

3.1.3.4 XRF

X-ray Fluorescence (XRF) Spectroscopy Signals were used to identify Sulfur peaks comes from CREKA and CREKA bound particles. This measurement was performed by using Bruker Tiger S8 XRF Spectrometer. All samples were prepared in powder form.

3.1.3.5 Nanodrop

Nanodrop is used to measure absorbance of CREKA, DOX intensities. In fibrin binding studies, CREKA amount did not bind to fibrin gel was characterized with CREKA absorbance by using NanoDrop2000 spectrometer (Thermo Scientific). To estimate loading efficiency of DOX to hydrogel particles, NanoDrop has been also used.

3.1.3.6 UV-VIS

In order to characterize DOX release profile, DOX absorbance at 390 nm was measured and fort his study UV-Visible (UV-VIS) Spectroscopy technique were utilized by using Shimadzı UV-3600- UV-VIS-NIR Spectrophotometer. All samples were 0.5 ml and glass cuvette was used for the measurements.

3.1.4 Fibrin Binding Assay

Fibrin gels were obtained in 96-well fluorescence microplate. In each well 30 µl fibrinogen solution and 20 µl thrombin solution were added. Solutions are incubated at 37 °C with shaking for 4 h. Then, 1 mg/ml PEG particles containing 0.5 mM, 1 mM CREKA, PEG particles and 0.5 mM, 1 mM CREKA peptide were incubated for 1h. Sample absorbance before incubation was recorded with NanoDrop2000 at 220 nm. After 1h incubation, unbound sample absorbance was obtained with NanoDrop2000 at 220 nm. Fibrin gel only condition was taken as control and its absorbance was subtracted from the rest. Each unbound group was normalized to its absorbance of total concentration. Each group has 3 replicates.

$$Bound\ Absorbance = 1 - \frac{Unbound\ Absorbance - Fibrin\ Absorbance}{Total(Inıtial)\ Absorbance}$$

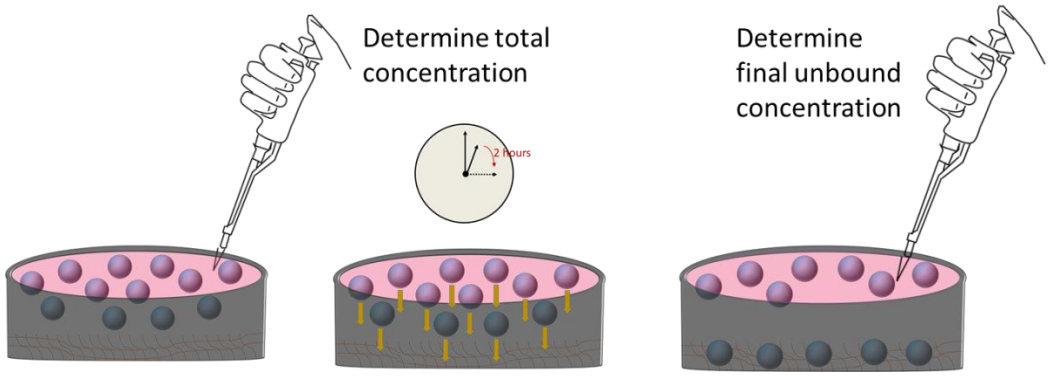

Figure 8. Schematics of Fibrin Binding Assay

3.1.5 DOX Loading & Release

Hydrogel particles were incubated with DOX in PBS in 10:1 ratio overnight. Unloaded DOX was removed with centrifugal filters. Hydrogel particles were loaded in cellulose membrane and membrane was incubated in 10 ml PBS at 37°C with gentle shaking. Samples were taken in every 30 minutes for 2 hours and every hour for next 4 hours and every 24 hours for next 120 hours in 500 µl. Each sample was replaced immediately with 500 µl PBS at 37 °C. Samples DOX absorbance at 390 nm was quantified with UV-VIS measurements in glass cuvettes with background of PBS. Loading efficiency and mass release profile was obtained with equations below [84, 85]:

$$Loading\ efficiency = (M0 - Mf)/Mf * 100 \quad (1)$$

$$Mt = Ct * V \sum Ct - 1 * Vs \quad (2)$$

$$\%Mass\ Release = (Mt - M\infty) * 100 \quad (3)$$

3.1.6 Cytocompatibility Tests

3.1.7 Cell Viability of HeLa Cervical Cancer Cell Line & BJ Human Dermal Fibroblast Cell Line

HeLa cervical cells were seeded 96 well fluorescence microplates at 5000 cells/well. After overnight incubation, medium in wells is removed and varying concentrations as 10 mg/ml, 5 mg/ml, 1 mg/ml, and 0.1 mg/ml as experimental groups were added to the cells in 80 µl/well medium in 3 replicates. The ATP amount was quantified with CTG reagent in 24 h and 72 h. ATP amount was normalized to control group of HeLa cells which does not include gels. For human dermal fibroblast cells, 10 mg/ml, 5 mg/ml, 1 mg/ml were also used as control groups to HeLa cells. For cytotoxicity evaluation of DOX loaded hydrogel particles 0.01 mg/ml of DOX was loaded overnight to 0.1 mg/ml hydrogel particles and incubated with cells for 24 h after removal of unloaded DOX with centrifugal filters.

3.1.8 Uptake Studies

3.1.8.1 24 Well Plate Preparation

Glass slides were autoclaved and placed in 24 well microplates. After then, 5000 cell/well of HeLa cells were added on glass slides in 500 μl DMEM and incubated overnight. In the meantime, gels were prepared with Dox loading since there is no fluorescence intensity would be had in confocal microscopy imaging without Dox molecules. Gel groups were incubated with DOX in PBS with a ratio of 10:1 (w/w) overnight. Unloaded DOX was removed via centrifugal filter 10 min 2500 rpm. DOX loading wad quantified with the ratio of absorbance after centrifuge to absorbance before centrifuge. Absorbance was measured with NanoDrop1000 at 390 nm.

DOX loaded PEG hydrogel particles were suspended in complete DMEM and replaced with well complete DMEM once cells were incubated overnight. Cells were incubated with DOX loaded gels for 1 h, then medium was removed and each well was washed with PBS 1x three times. After %4 formaldehyde in PBS was added to wells in 250 µl, incubated for 40 mins at 37°C. After incubation formaldehyde was removed and each well was washed with 250 µl PBS two times. Then %0.1 Triton-X was added in each well and incubated at room temperature for 5 min for permeabilization. After incubation, each well was washed with 250µl PBS two times. DAPI stock solution that was solved in PBS in a ratio of 1:1 added in each well 150 µl incubated 5 min at dark at room temperature. Finally each well was washed with 250 µl PBS, excess buffer was removed and glass covers were mounted on slides.

3.1.8.2 Imaging

Prepared samples on glass slides were examined with Scanning Fluorescence Confocal Microscopy, with both 20x and 60x magnification with immersion oil. Gain and fluorescence intensity was kept constant. Each figure is average of several images that are auto taken.

3.1.8.3 Intensity Quantification with ImageJ Processing

Each image was processed with ImageJ software. All images were saved as Bitmap, each of them channel separated first and then, cells were examined separately. Integrated densities for cell and background were calculated three times. Background intensities multiplied by area were subtracted from cell integrated intensities. Scale bars were adjusted in ImageJ. The ratio of DOX/DAPI was obtained as an indicator of cellular uptake efficiency in this study.

$$Intensity\ per\ cell = Cell\ Integrated\ density - (Background\ Integrated\ Density * Cell\ area)$$

3.1.8.1 Morphology Imaging with SEM

Cells were plated on glass slides in 24 well as 5000 cells/ well. Hydrogels as 0.1mg/ml concentration were incubated with cells for 1 h. The mediums were removed and cells were washed with PBS for 3 times. 4% glutaraldehyde was used for fixation of cells and cells were incubated with glutaraldehyde for 30 min at RT. After removing glutaraldehyde and washing the cells with PBS for 2 times, 0.1% osmium tetroxide was added onto cells and incubated for 30 min. Cells were washed with PBS twice and dehydrated with 30%, 50% 70% and 100% ethanol. In each step, cells were incubated for 5 minutes with degrees of ethanol. The glass slides were placed in filter paper and taken to critical point dryer with 40 °C and 112 bars for 1h. These samples were 10 nm gold coated and imaged with SEM.

Chapter 4

RESULTS & DISCUSSION

4.1 FE-SEM Imaging and Dynamic Light Scattering

FE-SEM imaging was performed to verify the formation of PEG hydrogel particles. It is also used to identify the size and size distribution of the hydrogel particles. All samples were characterized in powder form with 10 nm Au coating and 1 keV excitation energy.

Particle formation can be observed for each condition in Figure 9. Sizes of particles were altered in different samples, and it was observed from SEM images that particles within range of 40 nm - 5μm were present. According to DLS data, there were smaller particles (16 nm), which wouldn't be observed in FE-SEM and requires TEM (Figure 11). After all optimizations in synthesis, all particles are spherical, and some of them collide due to high intensity during polymerization (Figure 11). In SEM figures, the layers belonged to dextran sheets, which were buried within the structure of hydrogel particles. The surface of the hydrogel particles thus would be covered by dextran molecules. Peptide incorporation did not interfere with particle formation and gelation mechanism (Figure 9 and Figure 11).

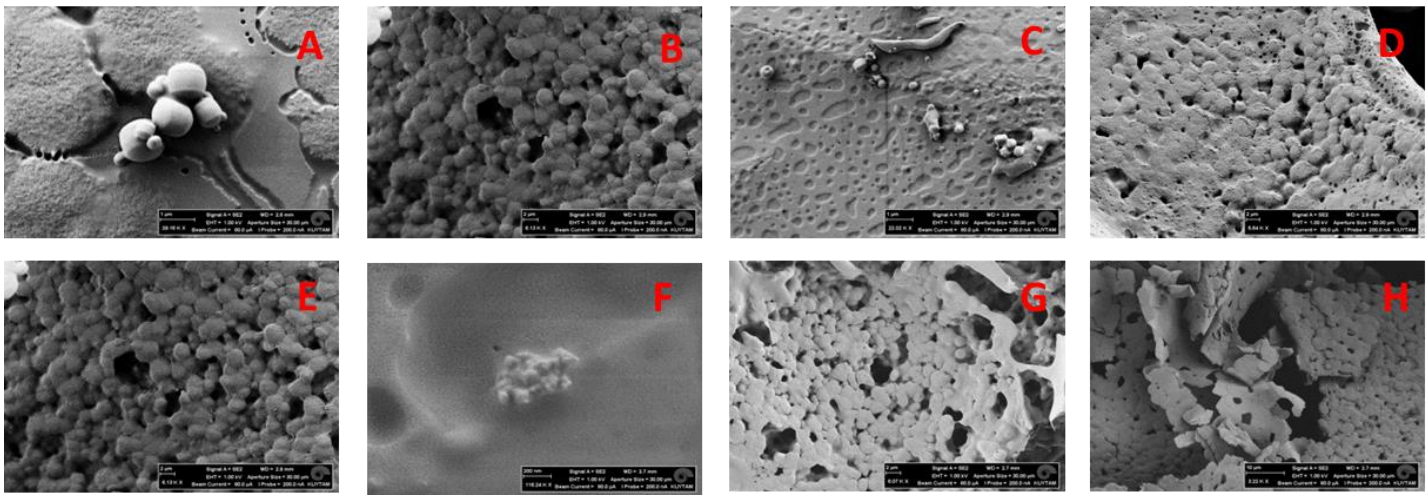

Figure 9. SEM images of nanogels containing A) PEG hydrogel B) CREKA conjugated PEG hydrogel C) RGDS conjugated PEG hydrogel D) IKVAV conjugated PEG hydrogel E) CREKA and RGDS conjugated PEG hydrogel F) CREKA and IKVAV conjugated PEG hydrogel G) RGDS and IKVAV conjugated PEG hydrogel H) CREKA, RGDS and IKVAV conjugated PEG hydrogel.

Table 1. DLS results of size distribution of PEG Hydrogel Particles

	Size (d.nm)	**% Intensity**	**St. Dev (d.nm)**
Peak 1	16.82	62.6	±7.336
Peak 2	262.5	29.7	±133.4
Peak 3	5045	7.7	±615.7

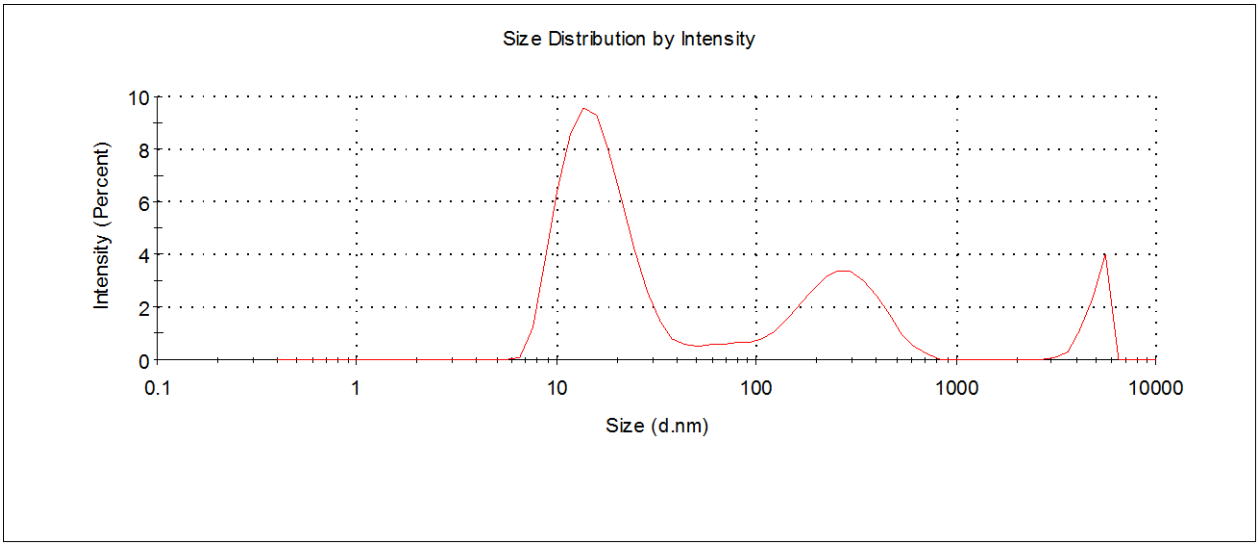

Figure 10. Size distribution of hydrogel particles

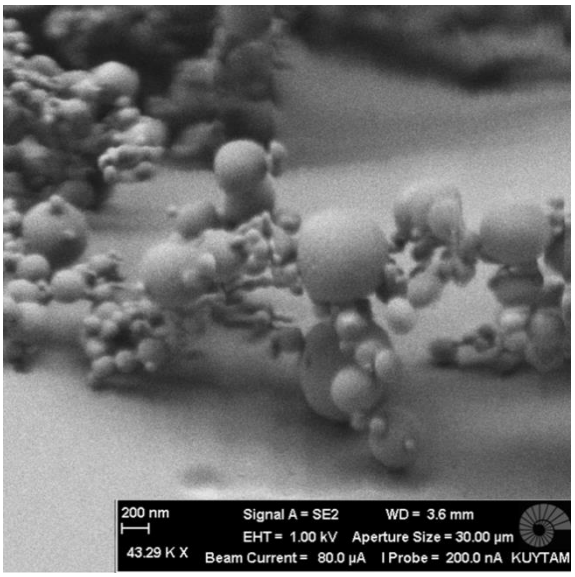

Figure 11. Scanning electron microscope (SEM) image of CREKA coated nanogels

To prevent incorporation of dextran onto the surface of hydrogel particles, several parameters were studied (Figure 12). Dextran buffer solution that consisted of several salts to solve dextran molecules was prepared at pH 8. Since dextran has OH and bulky structure, it may form hydrogen bonding in solvent causing precipitations[86] on hydrogel particles, and when dried it may result in dextran sheets. In order to break the dextran sheets, dextran solution was sonicated for few hours before microemulsion. With sonication time, pH of buffer solution that was used to solve dextran was also optimized. Since pH also contributes to H bonding between dextran groups, buffer solutions at different pH values were studied. pH 2 and 12 compromised the formation of microemulsion, where pH 4 and 10 affected less the emulsion and gelation mechanism. Best results were obtained at pH 6 and 8, with longer sonication times. The hydrogel particles that are obtained at pH 6 were slightly better dispersed and free from dextran. Slightly acidic pH was sufficient to disturb the level of H bonding as well as not disturbing emulsion and gelation mechanism, since in order to crosslink the system pH 8 was crucial for hydrogel particles after formation via microemulsion method. Small fragments of dextran were obtained with increased sonication times. Hence, hydrogel particles were separated from dextran molecules.

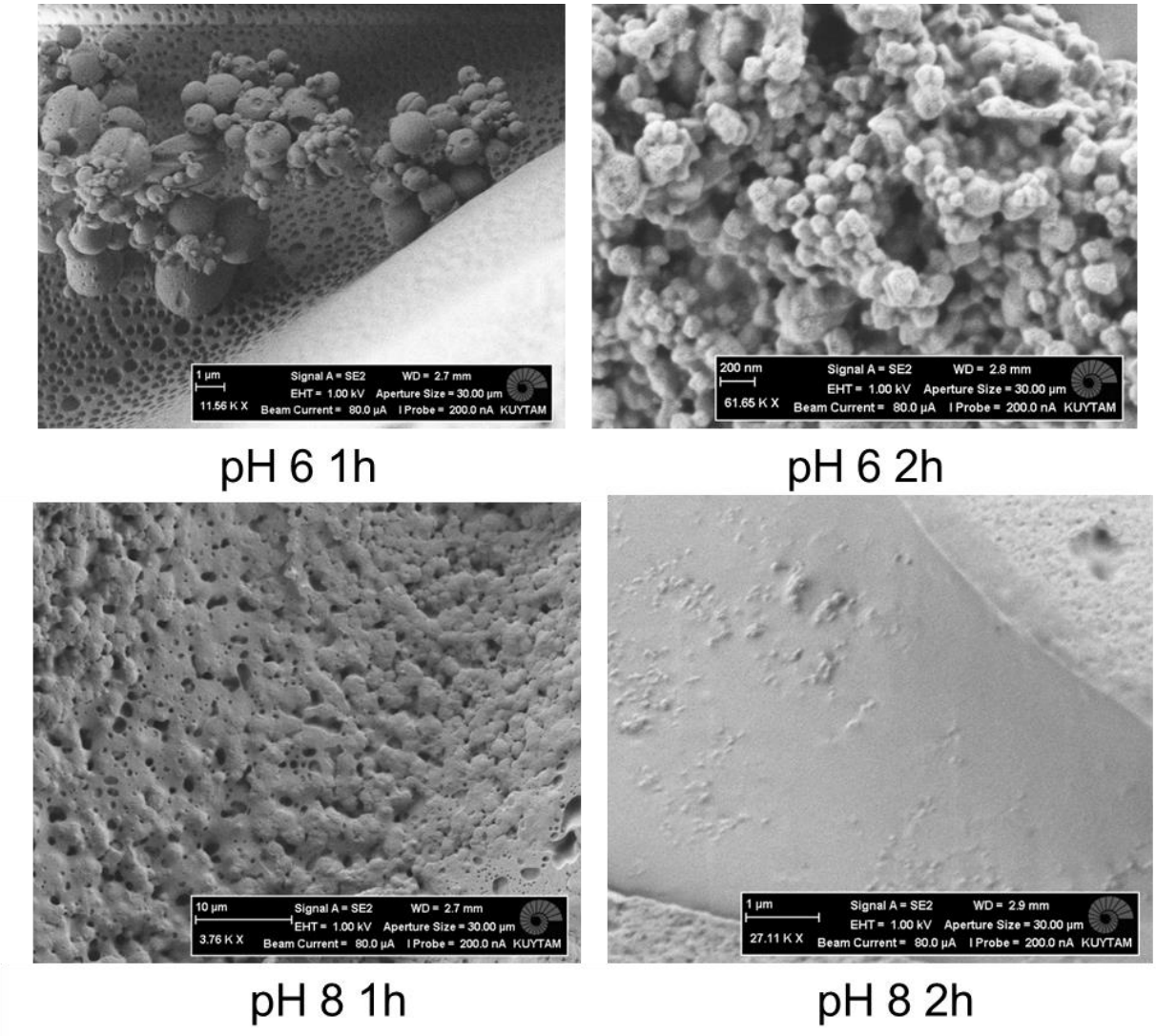

Figure 12. Hydrogel particles at different pH and sonication

4.2 FT-IR and XRF Spectroscopy

FT-IR and XRF were carried out to demonstrate conjugation of peptides to hydrogel structure. CREKA was incorporated via thiol ether linkage to acrylate groups in PEG diacrylate, where RGDS and IKVAV peptides were conjugated to SVA-PEG-acrylate (3400 Da) through the reaction of SVA with amine group. Since these conjugates have acrylate groups, these would be covalently cross-linked to PEG hydrogels. Peptide conjugation to SVA-PEG-Acrylate groups from SVA group was confirmed with FT-IR spectroscopy. Bonds between acr-PEG-SVA and peptide could be identified with either infrared or Raman spectroscopy. Conjugation of CREKA into the hydrogel network could be identified by XRF.

FT-IR analysis of RGDS and IKVAV conjugates with 3400 Da Acrylate-PEG-SVA, (Figure 13 and Figure 14) showed that, the peak at 648 cm^{-1} appeared due to the N-H stretching of imide in SVA. This peak disappeared in acrylate-PEG-Peptide conjugate spectra as a result of amide bond formation between SVA and carboxylic group of the peptide. Between 750 and 1250 cm^{-1} characteristic peaks appeared from PEG could be identified. For example, 1720 cm^{-1} peak of C=O represents the backbone chain in PEG. Formation of amide bonds in RGDS and IKVAV conjugates were confirmed at 1630 cm^{-1}. At 1630 cm^{-1} where it appeared due to NH_2 scissoring that is in the structure of peptide and amide C-N bond respectively. On the other hand, with imide ring stretching at 648 cm^{-1}, 1780 cm^{-1} and 1810 cm^{-1} peaks comes from C=O peaks[87] due to SVA group were disappeared, showing that conjugation reaction completed successfully.

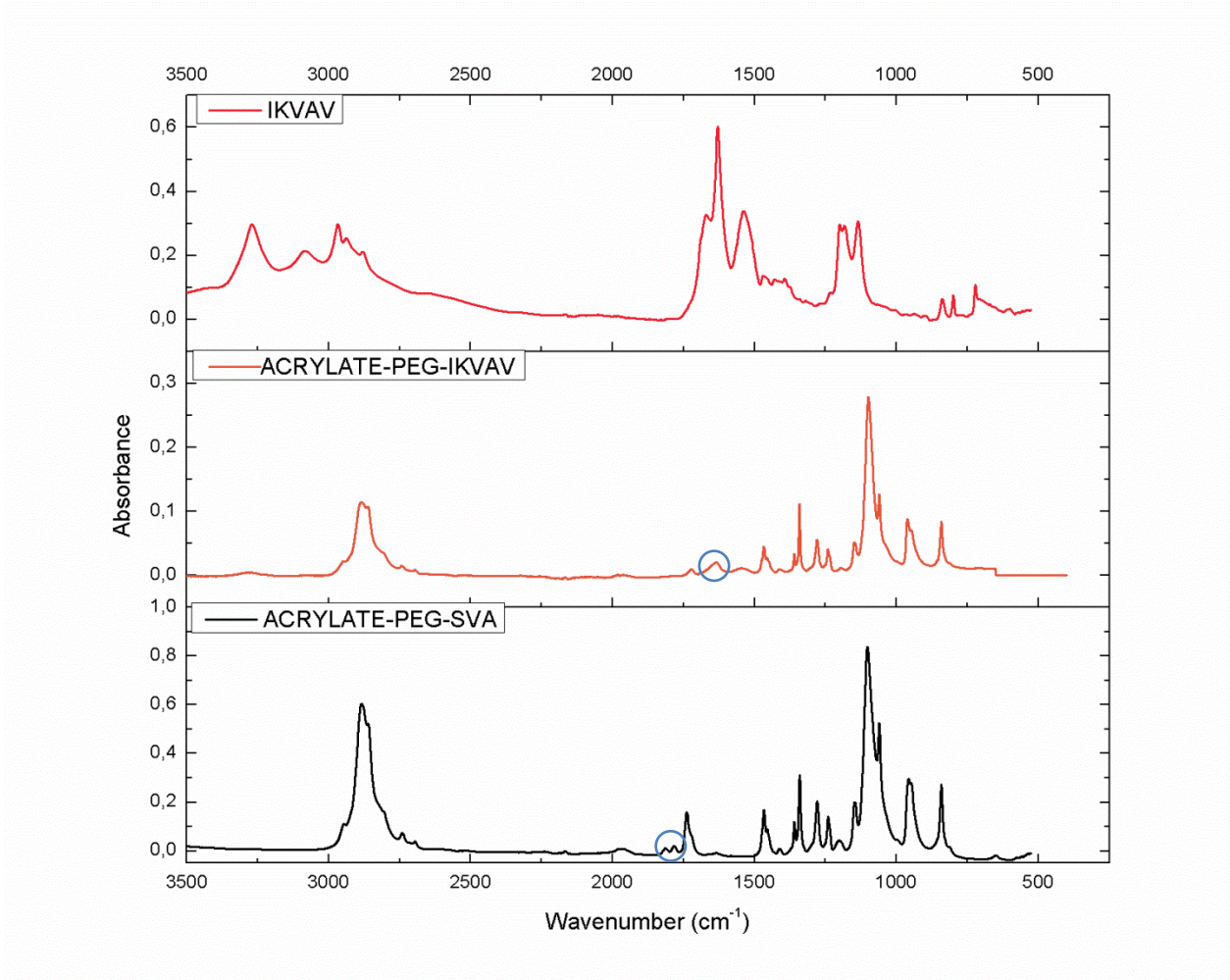

Figure 13. FT_IR Spectra of IKVAV, Acrylate-PEG-IKVAV and Acrylate-PEG-SVA Structures

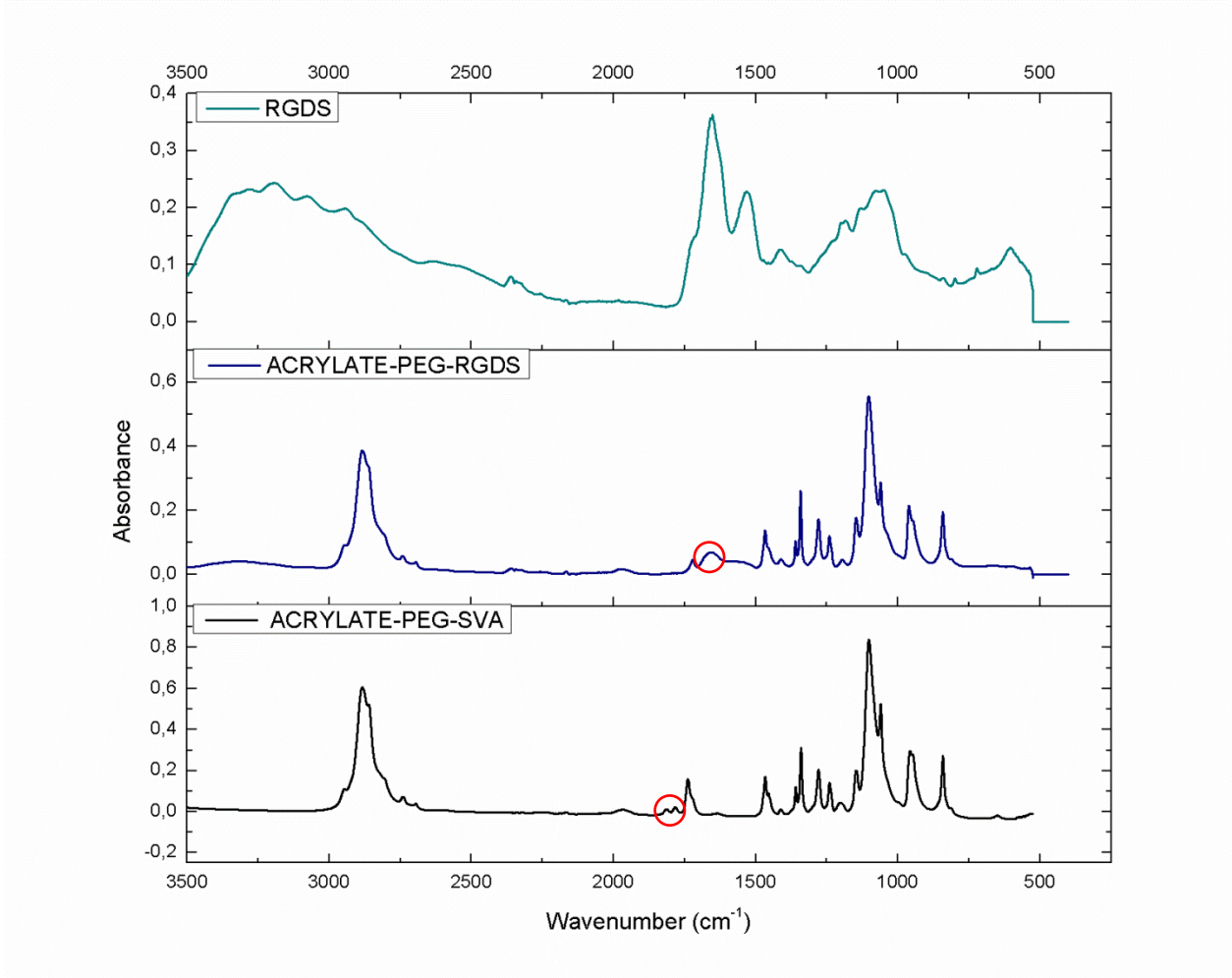

Figure 14. FT-IR Spectra of RGDS, Acrylate-PEG-RGDS, Acrylate-PEG-SVA Structures

For peptide conjugated samples such as IKVAV-PEG and RGDS-PEG hydrogels, there is a characteristic shoulder at 1640 cm^{-1} that comes from amide bonding. The peaks at 1484 and 1150 cm^{-1} correspond to N-H bending, C-N stretching and C-C stretch that also known for characteristics of Amide II and Amide III bonds in peptide sequences [88]. The shoulders in these regions are not present in plain PEG hydrogel sample.

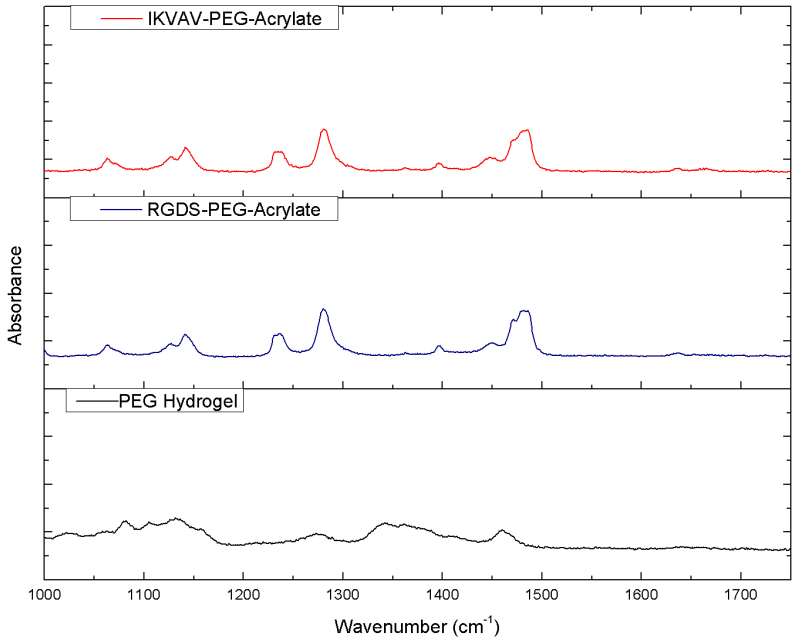

Figure 15. Raman spectra of conjugated peptides of IKVAV, RGDS and PEG Hydrogel

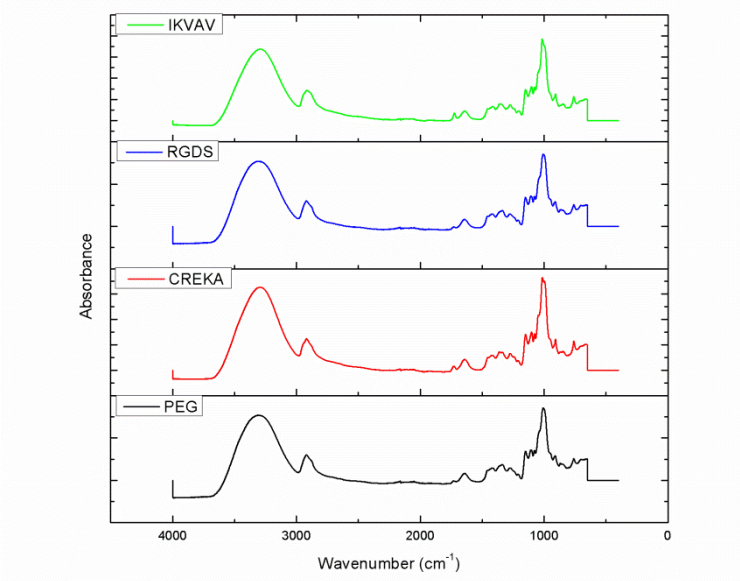

Figure 16. FT-IR spectra of IKVAV, RGDS, CREKA incorporated PEG Hydrogel Particles

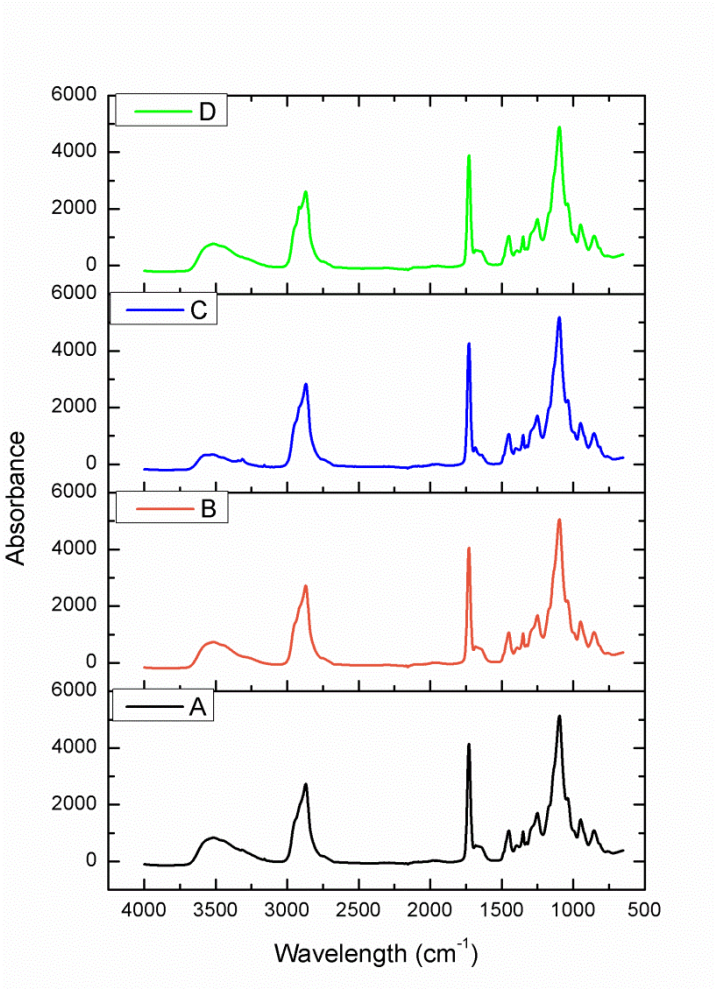

Figure 17. Fourier transform infrared spectra of **A)** PEG Gel **B)** CREKA-PEG Gel **C)** RGDS-PEG Gel **D)** IKVAV-PEG Gel

Since all hydrogels were washed with centrifugal filters that had a molecular weight cutoff of 10000 Da, all unconjugated peptides within hydrogel samples were expected to be removed from the system upon rinsing. Because dextran residues were observed in hydrogels, dextran interfered with PEG hydrogels in both Raman and infrared spectroscopy due to its aromatic groups and phenol signals (Figure 5).

XRF results showed the sulfur K_α peak at 2.307 keV, K_β peak at 2.485 keV labeled with pink vertical line, where sulfur atom coming from CREKA was present. Above the baseline (shown with blue line), sulfur peak at Kα could be identified for each sample that contained CREKA (Figure 18). However, only PEG hydrogel sample did not have any peak at 2.307 KeV, confirming the absence of CREKA in the structure (Figure 18). On the other hand, Kβ could not be observed, probably due to the X-ray signal noise that occurred from dextran and PEG. The results demonstrated that conjugation of CREKA peptides was successful, and that covalent conjugation through thiol-acrylate occurred.

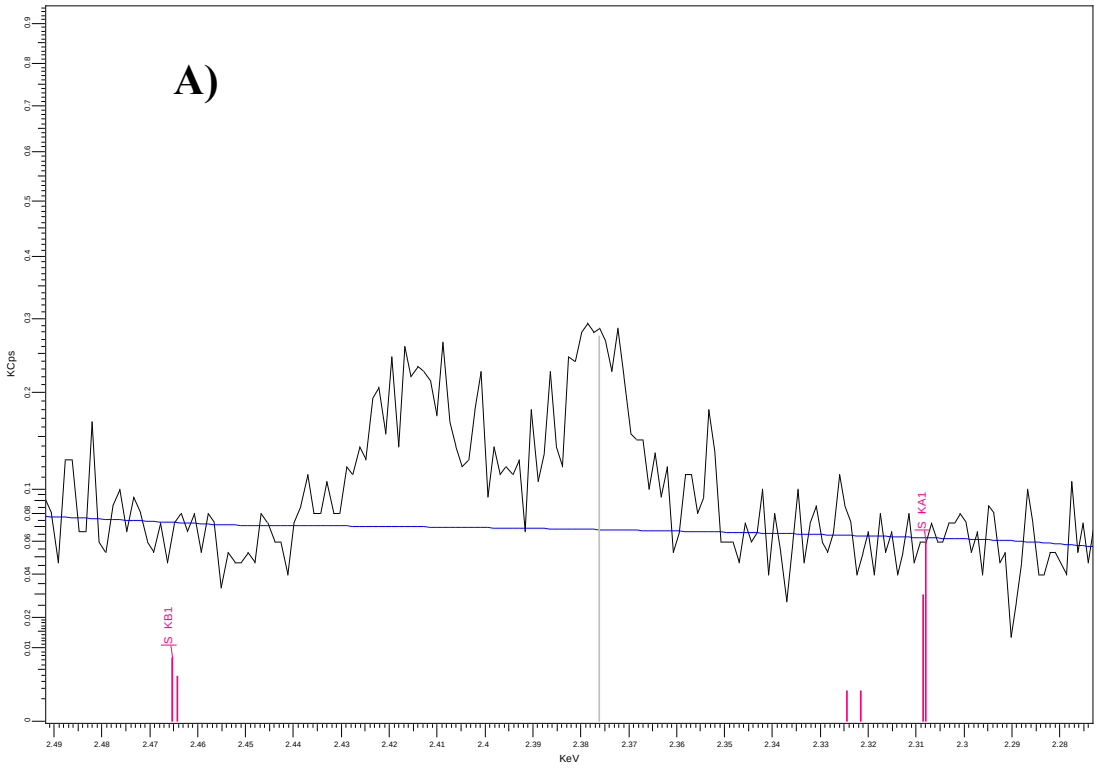

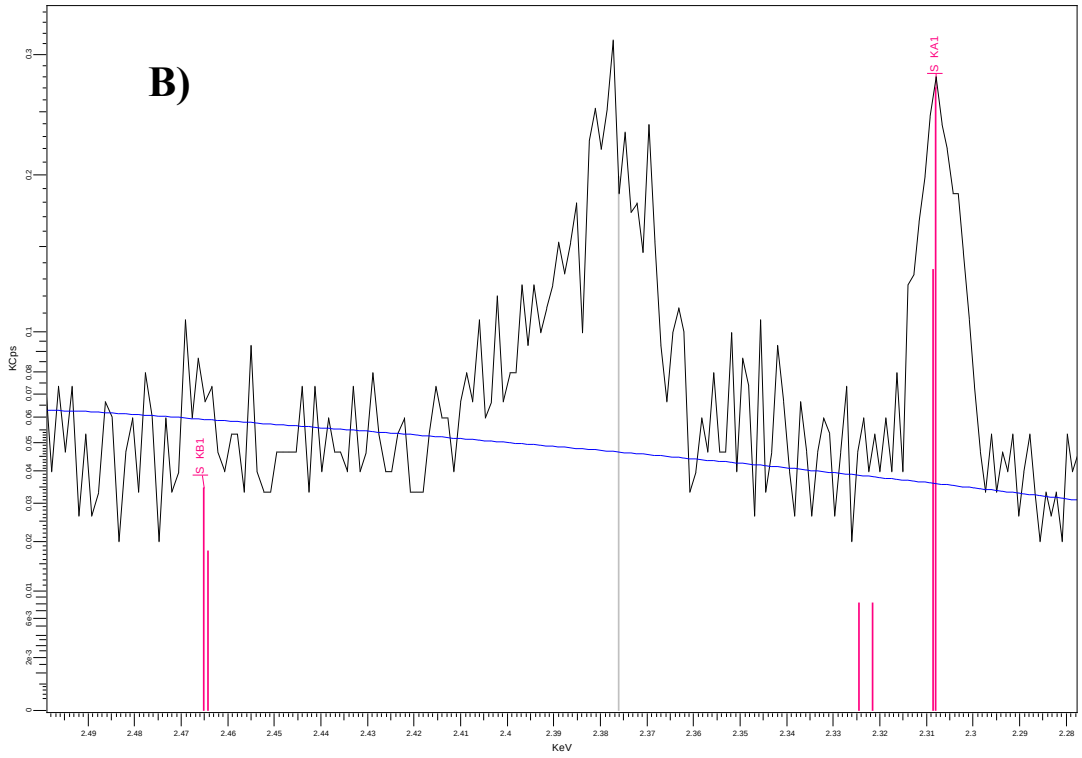
B)
S KA1
S KB1
KCps
KeV

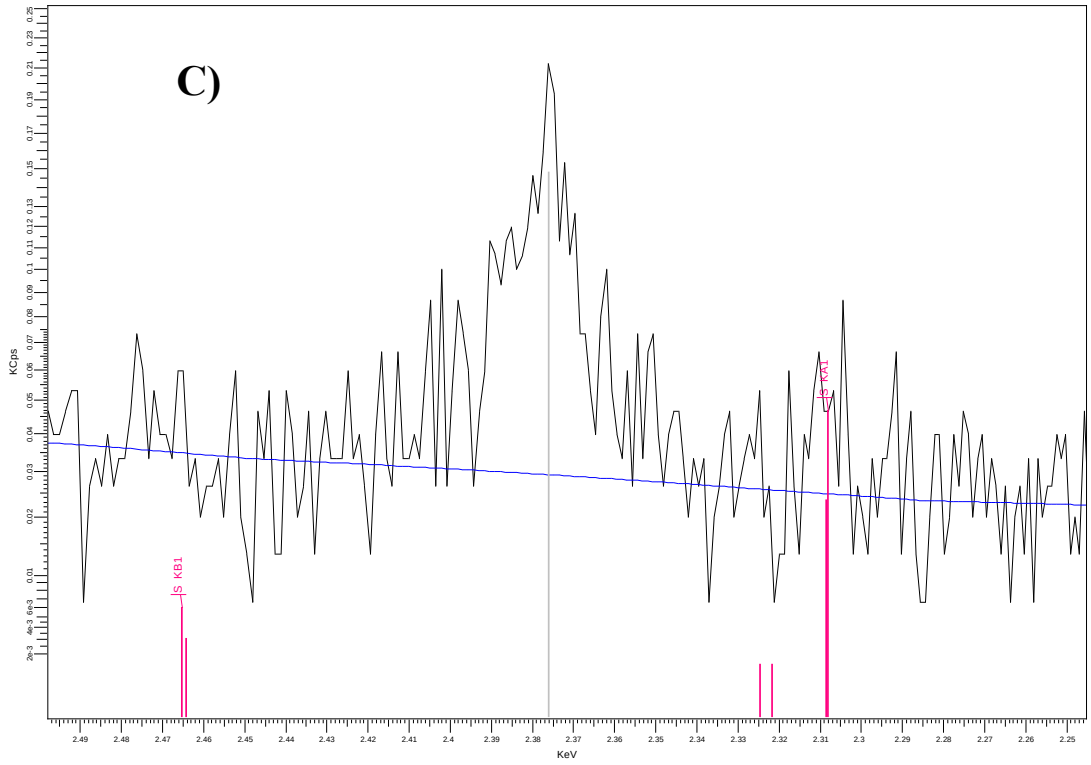
C)
KCps
KeV
S KB1
S KA1

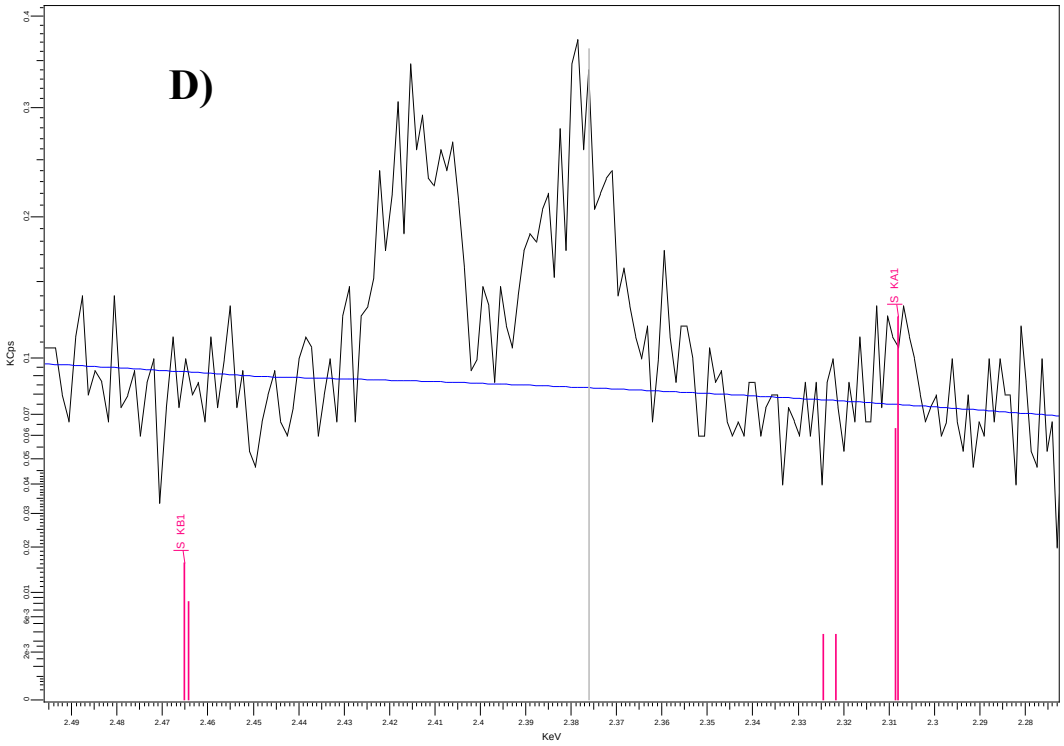
D)
KCps
KeV
S KB1
S KA1

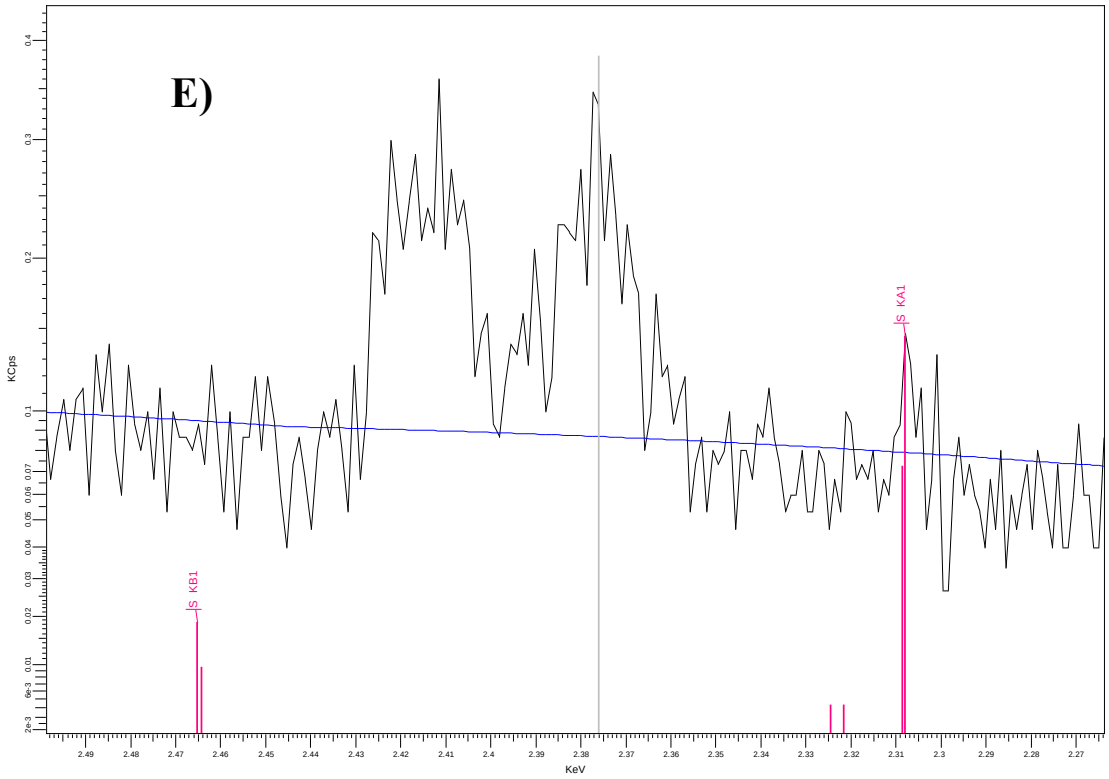

Figure 18. XRF Spectra of A) PEG Hydrogel Particle B) CREKA Conjugated PEG Hydrogel Particle C) CREKA and RGDS Conjugated PEG Hydrogel Particle D) CREKA and IKVAV Conjugated PEG Hydrogel Particle E) CREKA, RGDS and IKVAV Conjugated PEG Hydrogel Particle

4.3 Fibrin Binding Assay

CREKA is a pentapeptide, which has been demonstrated as tumor homing peptide [7]. It targets fibrin structure that is generously found in tumor environment [5]. CREKA can target collagen IV, present within fibrin [79], and normally found in extracellular matrix of endothelial cells. However, once the region transform to tumor region, endothelial cells overexpress collagen IV leading to increase in amount of this part of extracellular matrix.

In order to demonstrate the influence of CREKA incorporation into hydrogel networks on fibrin capacity, fibrin binding assay was used. This assay allowed us to quantify and compare CREKA binding and CREKA conjugated PEG hydrogel particle binding onto fibrin gel structure [7, 89]. In this study, CREKA absorbance was measured at 220 nm with concentrations of 0.5 mM and 1 mM. Same concentrations of CREKA were incorporated into PEG hydrogel particle structures in altered groups. PEG hydrogel particles without CREKA were also incubated with fibrin gel.

While 70% of freely CREKA peptides could bind to fibrin, PEG hydrogel particles without CREKA incorporation demonstrated 45% of binding affinity to fibrin gel, suggesting that PEG and Dextran might have contributed to fibrin binding. CREKA conjugated PEG hydrogel particles demonstrated higher affinity to fibrin compared to only CREKA peptide. PEG hydrogel particles with 0.5 mM CREKA conjugation demonstrated 94% affinity to fibrin binding; hence the experiments were continued with 0.5mM CREKA peptide that is involved in PEG hydrogel prepolymer solution.

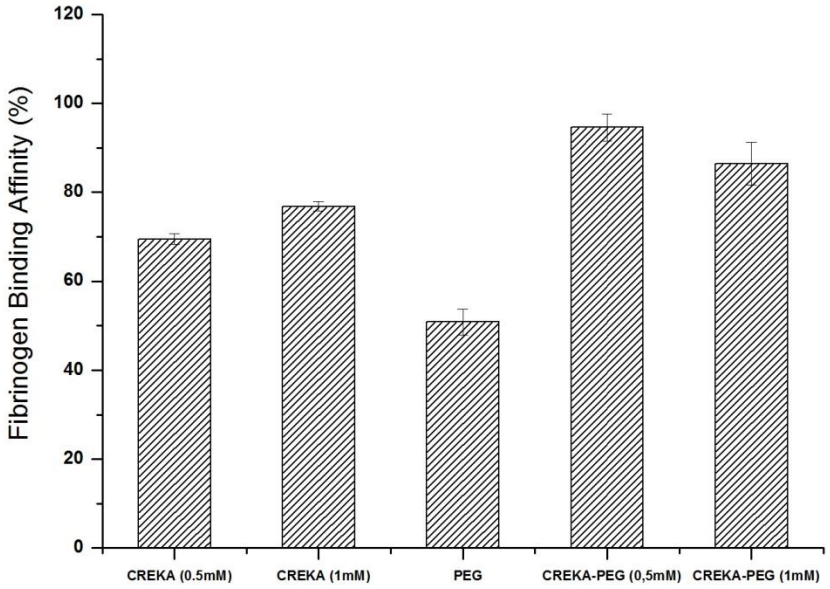

Figure 19. Fibrin binding affinity of PEG and CREKA conjugated PEG hydrogel particles. Gels and peptides with CREKA concentrations of 0.5 mM and 1 mM were incubated with 4 h on fibrin gel at 37°C. CREKA absorbance at 220 nm were measured with Nanodrop (Experiments were repeated at least 3 times)

4.4 Doxorubicin (DOX) Release from PEG Hydrogel Particles

DOX release experiments were carried out to characterize the release profile of the drug from PEG hydrogel particles synthesized via micro emulsion method. First, PEG hydrogel particles (1mg/ml) were incubated with 10:1 DOX to PEG hydrogel particle ratio overnight. Unloaded DOX was removed through centrifugation and release experiments were carried out. Loading efficiency of DOX to PEG hydrogel particles without peptides was measured as 40%. Release experiments were conducted for 100 hours. About 40% of the released drug was released during the first 10 hours. High release of DOX during the initial phases of the experiment could be explained by the release of a hydrophobic drug from a hydrophilic gel network [90] (Figure 20).

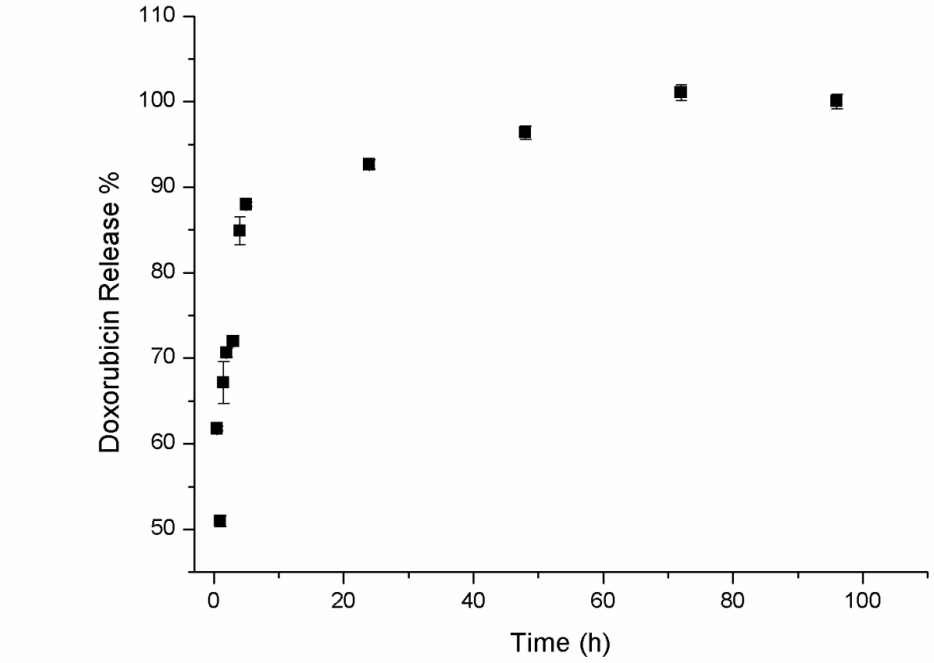

Figure 20. Cumulative DOX release profile. PEG hydrogel particles (1mg/ml) are incubated with 0.1 mg/ml DOX overnight, and released in PBS. DOX absorbance at 390 nm were measured with UV-Vis. (n=3)

4.5 Cytotoxicity Assay

To characterize the toxicity of hydrogel particles containing different peptide groups, HeLa cells were incubated with hydrogel particles in altered groups, where PEG hydrogel particle concentrations of 10 mg/ml, 5 mg/ml, 0.1 mg/ml and 0.01mg/ml were used. As a control group, healthy cells, human dermal fibroblasts (BJ cell line), were also incubated with PEG hydrogel particles. Cytotoxicity of cells in altered groups was measured with Cell-Titer-GLO luminescent viability assay on day 1 and day 3. The results were normalized with respect to control groups, where HeLa cells were not incubated with hydrogel particles. The viability results showed that concentrations of 0.1 mg/ml and 0.01 mg/ml were not cytotoxic, since these did not cause any decrease in viability of the treated HeLa and dermal fibroblast cells in three days [91]. However, 5 mg/ml and 10 mg/ml particle concentrations showed significant decreases in HeLa cell survival, suggesting the toxicity of particles on cells. Based on these results, 0.1 mg/ml or lower particle concentrations were considered as biocompatible for this system (Figure 21, Figure 22).

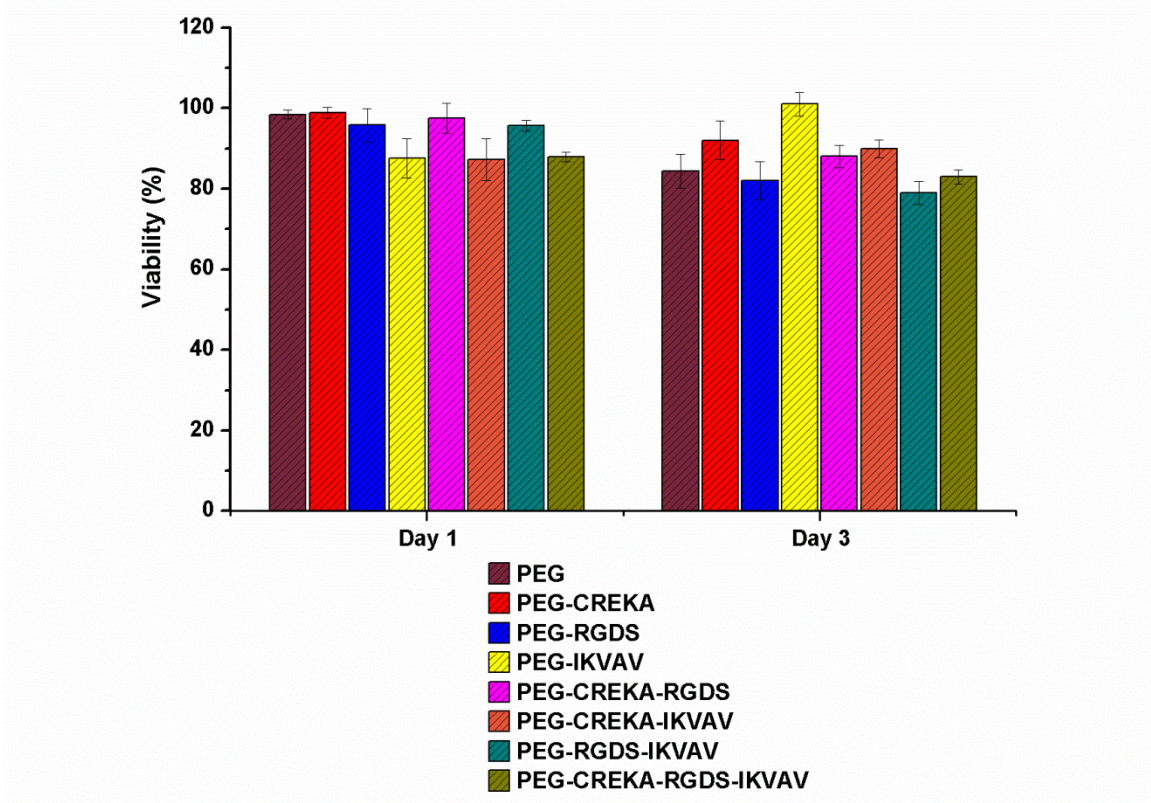

Figure 21. Cell viability on HeLa cell line in presence of **A)** PEG Gel **B)** CREKA conjugated PEG gel **C)** RGDS conjugated PEG gel **D)** IKVAV conjugated PEG gel **E)** CREKA and RGDS conjugated PEG gel **F)** CREKA and IKVAV conjugated PEG gel **G)** RGDS and IKVAV conjugated PEG gel **H)** CREKA, RGDS and IKVAV conjugated PEG gel for 24 h and 72 h. 0.1 mg/ml nanogels containing 0.5 mM CREKA and 2.5 mM RGDS and IKVAV were incubated for overnight. Results are normalized to control as only HeLa cells (n=3)

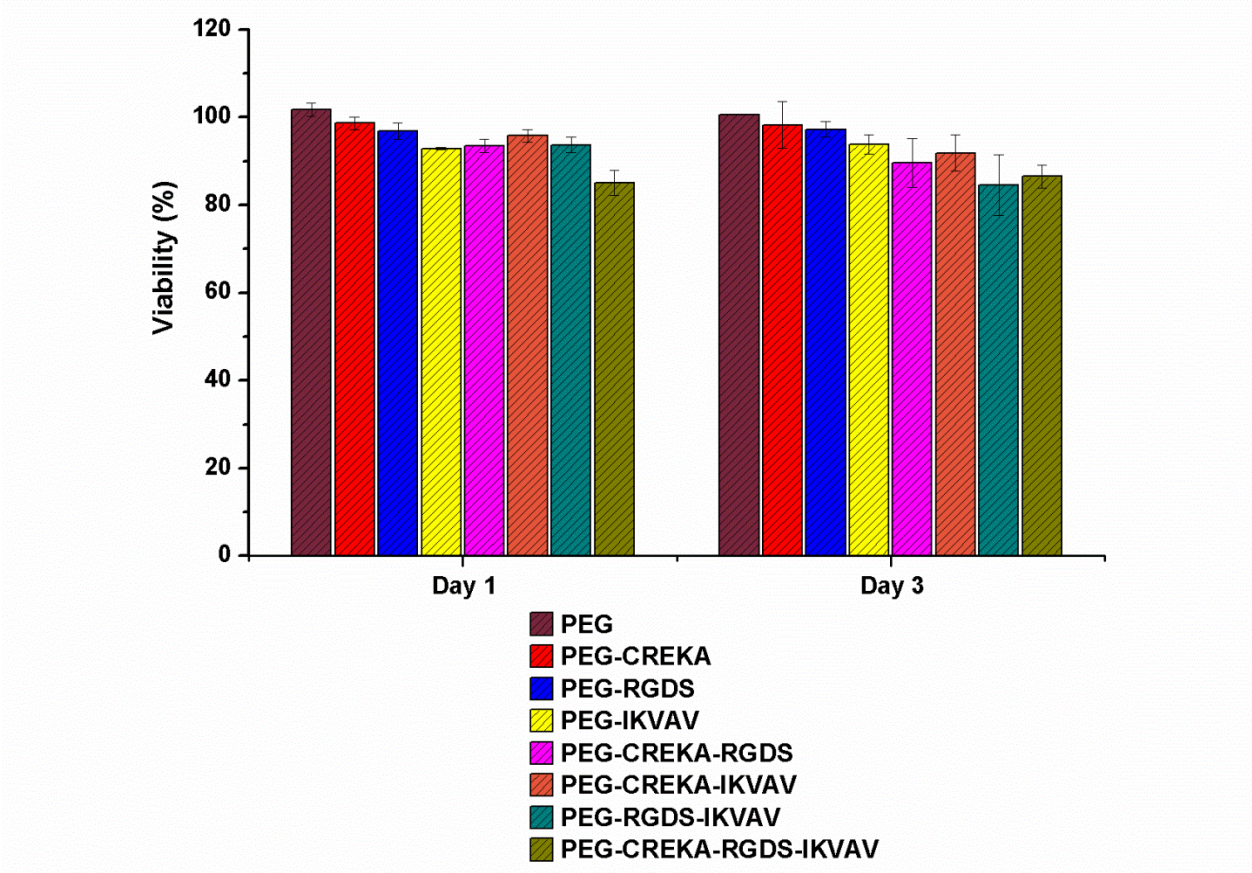

Figure 22. Cell viability on human fibroblast BJ cell line in presence of **A)** PEG Gel **B)** CREKA conjugated PEG gel **C)** RGDS conjugated PEG gel **D)** IKVAV conjugated PEG gel **E)** CREKA and RGDS conjugated PEG gel **F)** CREKA and IKVAV conjugated PEG gel **G)** RGDS and IKVAV conjugated PEG gel **H)** CREKA, RGDS and IKVAV conjugated PEG gel for 24 h and 72 h. 0.1 mg/ml nanogels containing 0.5 mM CREKA and 2.5 mM RGDS and IKVAV were incubated for overnight. Results are normalized to control as only BJ cells (n=3)

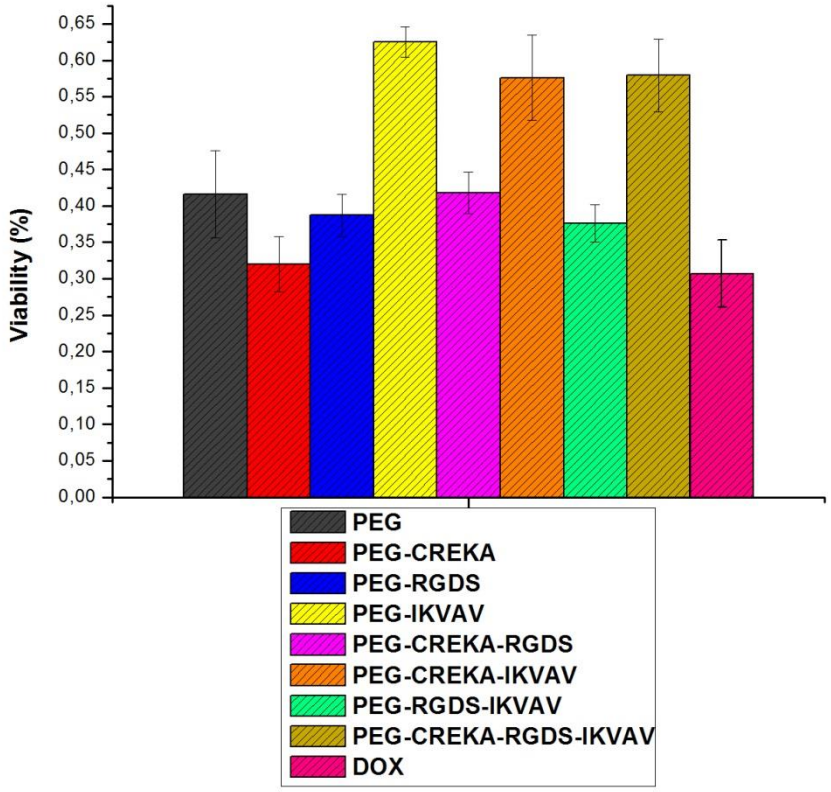

Figure 23. Cell viability on HeLa cell line in presence of DOX loaded **A)** PEG Gel **B)** CREKA conjugated PEG gel **C)** RGDS conjugated PEG gel **D)** IKVAV conjugated PEG gel **E)** CREKA and RGDS conjugated PEG gel **F)** CREKA and IKVAV conjugated PEG gel **G)** RGDS and IKVAV conjugated PEG gel **H)** CREKA, RGDS and IKVAV conjugated PEG gel **I)** HeLa cells for 24 h. Prior to cell treatment, 0.1 mg/ml nanogels containing 0.5 mM CREKA and 2.5 mM RGDS and IKVAV were incubated with 0.01mg/ml DOX overnight. Results are normalized to control as only HeLa cells (n=3)

4.5.1 Uptake Studies

Cellular uptake of PEG hydrogel particles by HeLa cells was investigated via confocal microscope. PEG hydrogel particles were loaded with DOX and fluorescence of DOX intensity was considered as a result of drug uptake into cells[69]. After 1h incubation of cells with DOX loaded hydrogel particles, cells were fixated with formaldehyde, and

stained with DAPI. DOX uptake by cells was measured with confocal microscope. Uptake degree was quantified as a ratio of DOX fluorescence intensity (red) to DAPI fluorescence intensity (blue) (Figure 25), where fluorescence intensities were measured based on images in Figure 24. DOX loaded HeLa cells were considered as a control group, and results in the rest of the groups (Figure 25) were normalized with respect to the DOX fluorescence in only DOX incubated HeLa cells.

CREKA, RGDS and IKVAV are known as targeting ligands, since these peptides consist of amino acids that mimic various parts of extracellular matrix proteins [92]. RGDS and IKVAV are mimicry of parts of laminin [93, 94]. Since RGDS and IKVAV target different regions of integrin [93, 94] and CREKA targets collagen IV in fibrin structure, their efficiency of targeting would differ. Significant differences in DOX uptake in CREKA incorporated PEG hydrogel group was observed compared to the other groups as was observed in both Figure 24 and Figure 25. In an earlier study, it was shown that HeLa cells transcribed Collagen IV as an extracellular matrix[95]. The successful result of CREKA in targeting in uptake experiments would be due to Collagen IV that was secreted by HeLa cells to outer environment. The overexpression and expression of $\alpha_v\beta_3$ integrin and nucleolin, which serves as a ligand for IKVAV as cell surface receptor proteins for RGDS and IKVAV, respectively in HeLa cell lines, were already presented in previous studies [70, 77]. These expressions of receptors would contribute to uptake of hydrogel particles containing RGDS and IKVAV.

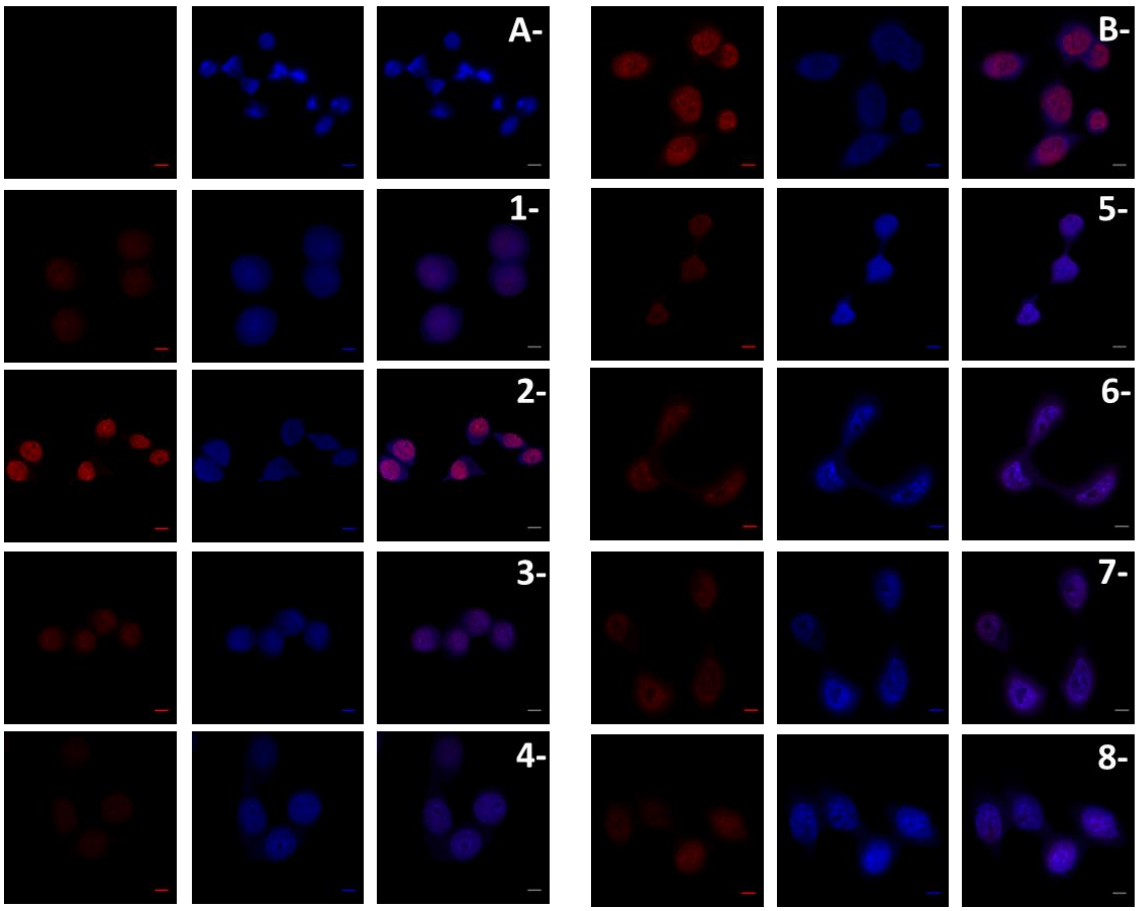

Figure 24. Cellular uptake levels of DOX loaded PEG hydrogel particles visualized by laser scanning confocal microscope. Increased cellular uptake with CREKA and RGDS conjugated PEG gel is confirmed with respect to conditions of **1)** PEG Gel **2)** CREKA conjugated PEG gel **3)** RGDS conjugated PEG gel **4)** IKVAV conjugated PEG gel **5)** CREKA and RGDS conjugated PEG gel **6)** CREKA and IKVAV conjugated PEG gel **7)** RGDS and IKVAV conjugated PEG gel **8)** CREKA,RGDS and IKVAV conjugated PEG gel. As control groups **A)** DOX only **B)** HELA only are used. 0.1 mg/ml gels are incubated with 0.01 mg/ml DOX for overnight. Cells were incubated with DOX loaded gel for 2 h. Images were taken after fixation and gels that are not internalized were removed by washing.

LEFT COLUMNS: (A,B-1:8): Overlay images of DOX fluorescence and DAPI staining.

RIGHT COLUMNS: 1a-8a DOX fluorescence (red) 1b-8b DAPI staining (blue), Scale bar =10 μm. (n=3)

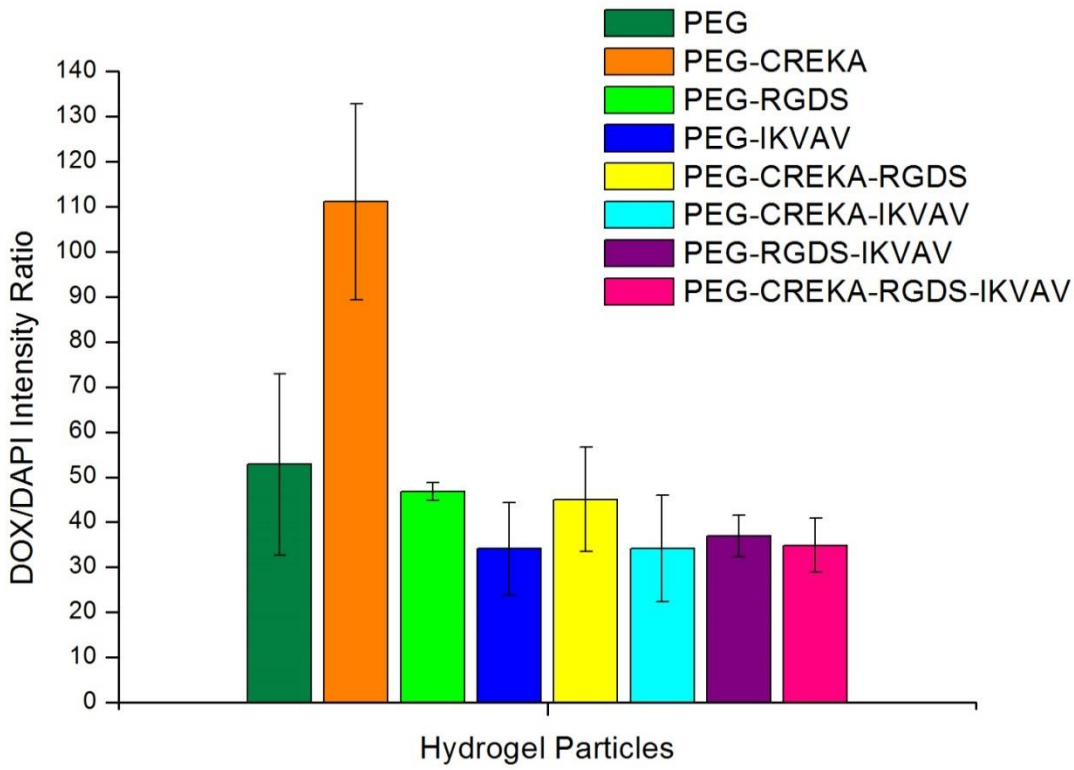

Figure 25. Quantification of fluorescence intensity ratio of DOX/DAPI based on laser scanning confocal microscopy images using ImageJ. (n=3)

In the absence of any peptide, DOX uptake of 50% was measured in HeLa cells. These results can be explained by dextran molecules that remained on particle surface, which would be expected to contribute to DOX uptake [96-98] . In peptide conjugated PEG hydrogel group, CREKA concentration in PEG hydrogel particles was 0.5 mM, where RGDS and IKVAV conjugate concentration of 2.4 mM was used in pre-polymer solution. Figure 25 suggested higher targeting capability of CREKA conjugated hydrogel particles to HeLa cells than that of RGDS and IKVAV conjugated groups. Both RGDS and

CREKA+RGDS conjugated hydrogel particle groups demonstrated slightly higher uptake into HeLa cells, compared to the groups where combination of peptides were used. This improved uptake with RGDS was also observed in previous studies from our group, which could be due to high amount of $\alpha_v\beta_3$ integrin receptors on HeLa cell surfaces [70, 85]. This result was supported with viability result when HeLa cells were treated with DOX loaded hydrogel particles functionalized with altered peptide groups. CREKA showed the least viability, suggesting the highest uptake caused more death in this group (Figure 23).

Despite significant increases in hydrogel uptake with only CREKA conjugation, incorporation of CREKA with other peptides into particle gel network did not result in significant uptake of particles by HeLa cells. This result could be due to lower accessibility of CREKA peptide by extracellular matrix when other peptides were also incorporated. CREKA was covalently conjugated into the network through thiol-acrylate reaction, where other peptides were conjugated into the network through the acrylate group of acrylate-PEG-peptide molecules. The presence of PEG chains might have allowed for improved accessibility of RGDS or IKVAV rather than CREKA, and might have blocked interactions of CREKA with Collagen IV which was transcribed by HeLa cells[99]. As a result of limited interaction of CREKA with its receptors in the presence of other peptides within the network, CREKA might not contribute to improved uptake compared to the condition where only CREKA was used.

Particle uptake was also characterized with SEM. Figure 26 shows HeLa cells with different magnifications treated with CREKA incorporated PEG hydrogel particles. According to these images, cells preserved their morphology, and that hydrogel particles were observed on surface of cells as an evidence of interaction between hydrogel particles and cells. HeLa cells that were not treated with hydrogel particle and treated with hydrogel particles were also compared and indicated similar morphology Figure 27.

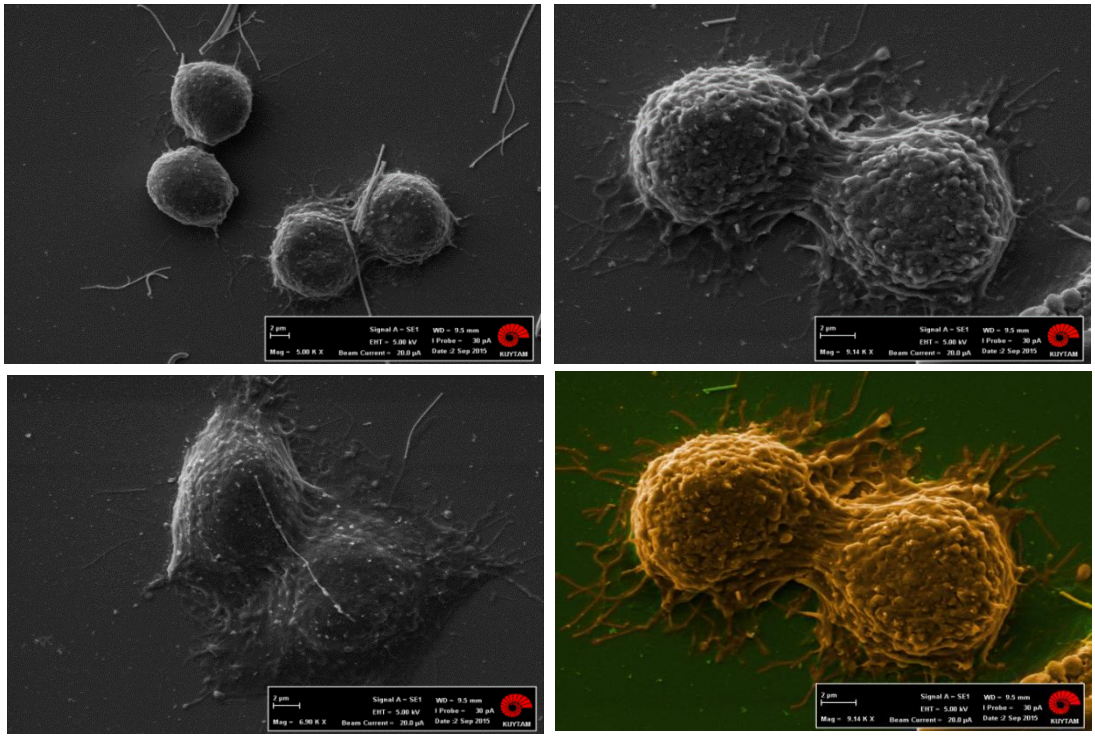

Figure 26. HeLa Cells treated with CREKA incorporated PEG Hydrogel Particles. Scale bar=2 µm

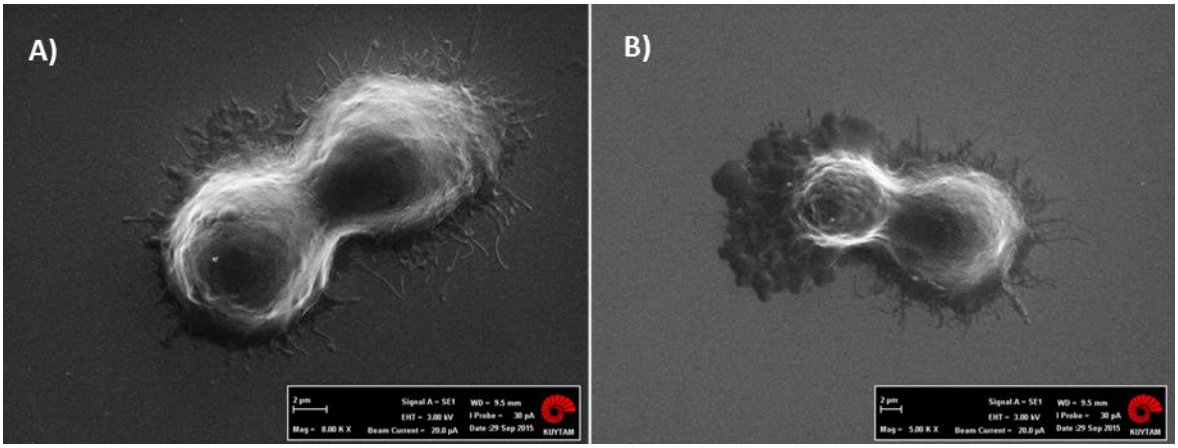

Figure 27. **A)** HeLa Cells only and **B)** HeLa Cells treated with CREKA incorporated PEG Hydrogel Particles. Scale bar = 2 µm

Chapter 5

CONCLUSION

In this study, the influence of multiple selective targeting ligands through the use of PEG hydrogel particles on targeting cancer cell surface and environment was studied. PEG based drug delivery vehicles were prepared via water-in-water emulsion technique in aqueous dextran solution. RGDS, IKVAV and cysteine–arginine–glutamic acid–lysine–alanine (CREKA) small peptides and/or combinations were conjugated to hydrogel particles as targeting ligands. Cell survival experiments carried out in the presence and absence of PEG hydrogels demonstrated higher viability for the cells treated with CREKA conjugated hydrogel particles. In addition, fibrin binding assay showed that CREKA conjugated particles can bind to fibrin with 94% binding affinity compared to particles in other groups, suggesting the targeting potential of PEG hydrogel particles through CREKA functionalization. Use of targeting ligands would overcome problems due to damage to healthy cells and decrease toxicity of drugs since targeting would definitely decrease the amount needed for efficient therapy. This study is promising for the development of targeted delivery vehicles, and provides the foundation of CREKA and RGDS/IKVAV mediated targeting of cancer cells For further studies, effect of CREKA with conjugated form to PEG chain would be studied, and addition of degradable peptide sequence into hydrogel prepolymer will be considered to design as an effective delivery vehicle.

BIBLIOGRAPHY

1. Ashley, C.E., et al., *The targeted delivery of multicomponent cargos to cancer cells by nanoporous particle-supported lipid bilayers.* Nat Mater, 2011. **10**(5): p. 389-397.
2. Irvine, D.J., *Drug delivery: One nanoparticle, one kill.* Nat Mater, 2011. **10**(5): p. 342-343.
3. Jin, S.E., H.E. Jin, and S.S. Hong, *Targeted delivery system of nanobiomaterials in anticancer therapy: from cells to clinics.* Biomed Res Int, 2014. **2014**: p. 814208.
4. Chen Weihsu, C., X. Zhang Andrew, and S.-D. Li, *Limitations and niches of the active targeting approach for nanoparticle drug delivery*, in *European Journal of Nanomedicine*. 2012. p. 89.
5. Chung, E.J., et al., *Fibrin-binding, peptide amphiphile micelles for targeting glioblastoma.* Biomaterials, 2014. **35**(4): p. 1249-56.
6. Karmali, P.P., et al., *Targeting of albumin-embedded paclitaxel nanoparticles to tumors.* Nanomedicine, 2009. **5**(1): p. 73-82.
7. Simberg, D., et al., *Biomimetic amplification of nanoparticle homing to tumors.* Proc Natl Acad Sci U S A, 2007. **104**(3): p. 932-6.
8. Wadia, J.S. and S.F. Dowdy, *Transmembrane delivery of protein and peptide drugs by TAT-mediated transduction in the treatment of cancer.* Adv Drug Deliv Rev, 2005. **57**(4): p. 579-96.
9. McCarthy, J.R. and R. Weissleder, *Multifunctional magnetic nanoparticles for targeted imaging and therapy.* Adv Drug Deliv Rev, 2008. **60**(11): p. 1241-51.
10. Richard, C., M. de Chermont Qle, and D. Scherman, *Nanoparticles for imaging and tumor gene delivery.* Tumori, 2008. **94**(2): p. 264-70.
11. Opanasopit, P., et al., *Development and characterization of pectinate micro/nanoparticles for gene delivery.* AAPS PharmSciTech, 2008. **9**(1): p. 67-74.
12. Cherukuri, P., E.S. Glazer, and S.A. Curley, *Targeted hyperthermia using metal nanoparticles.* Adv Drug Deliv Rev, 2010. **62**(3): p. 339-45.
13. Accardo, A., D. Tesauro, and G. Morelli, *Peptide-based targeting strategies for simultaneous imaging and therapy with nanovectors.* Polymer Journal, 2013. **45**(5): p. 481-493.
14. Kikkawa, Y., et al., *Laminin-111-derived peptides and cancer.* Cell Adh Migr, 2013. **7**(1): p. 150-256.
15. Bresalier, R.S., et al., *THE LAMININ ALPHA-1 CHAIN ILE-LYS-VAL-ALA-VAL (IKVAV)-CONTAINING PEPTIDE PROMOTES LIVER COLONIZATION BY HUMAN COLON-CANCER CELLS.* Cancer Research, 1995. **55**(11): p. 2476-2480.
16. King, T.E., et al., *The role of alpha 6 integrin in prostate cancer migration and bone pain in a novel xenograft model.* PLoS One, 2008. **3**(10): p. e3535.

17. Whitelock, J.M., et al., *Multiple levels of post-transcriptional regulation of collagenase (matrix metalloproteinase 1) in an epithelial cell line.* Immunol Cell Biol, 1993. **71**(1): p. 39-47.
18. Nomizu, M., et al., *Structure-activity study of a laminin alpha 1 chain active peptide segment Ile-Lys-Val-Ala-Val (IKVAV).* FEBS Lett, 1995. **365**(2-3): p. 227-31.
19. Li, Y.-L., et al., *Reversibly Stabilized Multifunctional Dextran Nanoparticles Efficiently Deliver Doxorubicin into the Nuclei of Cancer Cells.* Angewandte Chemie International Edition, 2009. **48**(52): p. 9914-9918.
20. Laurent, S. and M. Mahmoudi, *Superparamagnetic iron oxide nanoparticles: promises for diagnosis and treatment of cancer.* Int J Mol Epidemiol Genet, 2011. **2**(4): p. 367-90.
21. Johannsen, M., et al., *Clinical hyperthermia of prostate cancer using magnetic nanoparticles: Presentation of a new interstitial technique.* International Journal of Hyperthermia, 2005. **21**(7): p. 637-647.
22. Gordon, A.C., et al., *Localized hyperthermia with iron oxide-doped yttrium microparticles: steps toward image-guided thermoradiotherapy in liver cancer.* J Vasc Interv Radiol, 2014. **25**(3): p. 397-404.
23. Laurent, S., et al., *Magnetic fluid hyperthermia: focus on superparamagnetic iron oxide nanoparticles.* Adv Colloid Interface Sci, 2011. **166**(1-2): p. 8-23.
24. Johannsen, M., et al., *Magnetic nanoparticle hyperthermia for prostate cancer.* Int J Hyperthermia, 2010. **26**(8): p. 790-5.
25. Cherukuri, P., E.S. Glazer, and S.A. Curley, *Targeted Hyperthermia Using Metal Nanoparticles.* Advanced drug delivery reviews, 2010. **62**(3): p. 339-345.
26. Sadhukha, T., T.S. Wiedmann, and J. Panyam, *Inhalable magnetic nanoparticles for targeted hyperthermia in lung cancer therapy.* Biomaterials, 2013. **34**(21): p. 5163-71.
27. Shah, B.P., et al., *Core-shell nanoparticle-based peptide therapeutics and combined hyperthermia for enhanced cancer cell apoptosis.* ACS Nano, 2014. **8**(9): p. 9379-87.
28. Liu, X., et al., *Gene therapy targeting glaucoma: where are we?* Surv Ophthalmol, 2009. **54**(4): p. 472-86.
29. Huschka, R., et al., *Gene silencing by gold nanoshell-mediated delivery and laser-triggered release of antisense oligonucleotide and siRNA.* ACS nano, 2012. **6**(9): p. 7681-7691.
30. Ibraheem, D., A. Elaissari, and H. Fessi, *Gene therapy and DNA delivery systems.* Int J Pharm, 2014. **459**(1-2): p. 70-83.

31. Toita, R., et al., *Protein kinase Cα-specific peptide substrate graft-type copolymer for cancer cell-specific gene regulation systems.* Journal of Controlled Release, 2009. **139**(2): p. 133-139.
32. Sakurai, F., H. Mizuguchi, and T. Hayakawa, *Efficient gene transfer into human CD34+ cells by an adenovirus type 35 vector.* Gene therapy, 2003. **10**(12): p. 1041-1048.
33. Shi, N. and W.M. Pardridge, *Noninvasive gene targeting to the brain.* Proceedings of the National Academy of Sciences, 2000. **97**(13): p. 7567-7572.
34. Fumoto, S., et al., *Targeted Gene Delivery: Importance of Administration Routes*. Novel Gene Therapy Approaches. 2013.
35. Tartaj, P., et al., *The preparation of magnetic nanoparticles for applications in biomedicine.* Journal of Physics D: Applied Physics, 2003. **36**(13): p. R182.
36. Neuberger, T., et al., *Superparamagnetic nanoparticles for biomedical applications: Possibilities and limitations of a new drug delivery system.* Journal of Magnetism and Magnetic Materials, 2005. **293**(1): p. 483-496.
37. Boutry, S., et al., *Specific E-selectin targeting with a superparamagnetic MRI contrast agent.* Contrast Media Mol Imaging, 2006. **1**(1): p. 15-22.
38. Serres, S., et al., *Molecular MRI enables early and sensitive detection of brain metastases.* Proceedings of the National Academy of Sciences, 2012. **109**(17): p. 6674-6679.
39. Cokol, M., et al., *Systematic exploration of synergistic drug pairs.* Molecular Systems Biology, 2011. **7**: p. 544-544.
40. Jawetz, E. and J.B. Gunnison, *Antibiotic synergism and antagonism; an assessment of the problem.* Pharmacol Rev, 1953. **5**(2): p. 175-92.
41. Langer, R., *New methods of drug delivery.* Science, 1990. **249**(4976): p. 1527-33.
42. Orive, G., et al., *Drug delivery in biotechnology: present and future.* Current Opinion in Biotechnology, 2003. **14**(6): p. 659-664.
43. Hu, C.M. and L. Zhang, *Therapeutic nanoparticles to combat cancer drug resistance.* Curr Drug Metab, 2009. **10**(8): p. 836-41.
44. Colombo, M., et al., *Biological applications of magnetic nanoparticles.* Chem Soc Rev, 2012. **41**(11): p. 4306-34.
45. Mashhadizadeh, M.H., *Drug-Carrying Amino Silane Coated Magnetic Nanoparticles as Potential Vehicles for Delivery of Antibiotics.* Journal of Nanomedicine & Nanotechnology, 2012. **03**(04).
46. Kievit, F.M., et al., *Doxorubicin loaded iron oxide nanoparticles overcome multidrug resistance in cancer in vitro.* J Control Release, 2011. **152**(1): p. 76-83.
47. Singh, R. and J.W. Lillard, Jr., *Nanoparticle-based targeted drug delivery.* Exp Mol Pathol, 2009. **86**(3): p. 215-23.

48. Nasongkla, N., et al., *cRGD-functionalized polymer micelles for targeted doxorubicin delivery.* Angew Chem Int Ed Engl, 2004. **43**(46): p. 6323-7.
49. Ahmad, Z., et al., *Polymeric micelles as drug delivery vehicles.* RSC Advances, 2014. **4**(33): p. 17028-17038.
50. Kataoka, K., A. Harada, and Y. Nagasaki, *Block copolymer micelles for drug delivery: design, characterization and biological significance.* Advanced Drug Delivery Reviews, 2001. **47**(1): p. 113-131.
51. Nasongkla, N., et al., *Multifunctional polymeric micelles as cancer-targeted, MRI-ultrasensitive drug delivery systems.* Nano Letters, 2006. **6**(11): p. 2427-2430.
52. Savic, R., et al., *Assessment of the integrity of poly(caprolactone)-b-poly(ethylene oxide) micelles under biological conditions: a fluorogenic-based approach.* Langmuir, 2006. **22**(8): p. 3570-8.
53. Bae, Y., et al., *Design of environment-sensitive supramolecular assemblies for intracellular drug delivery: Polymeric micelles that are responsive to intracellular pH change.* Angewandte Chemie-International Edition, 2003. **42**(38): p. 4640-4643.
54. Gulati, M., et al., *Lipophilic drug derivatives in liposomes.* International Journal of Pharmaceutics, 1998. **165**(2): p. 129-168.
55. Immordino, M.L., F. Dosio, and L. Cattel, *Stealth liposomes: review of the basic science, rationale, and clinical applications, existing and potential.* International Journal of Nanomedicine, 2006. **1**(3): p. 297-315.
56. Grit, M. and D.J. Crommelin, *Chemical stability of liposomes: implications for their physical stability.* Chem Phys Lipids, 1993. **64**(1-3): p. 3-18.
57. *Mechanics and physics of hydrogels.* Soft Matter, 2012. **8**(31): p. 8006-8007.
58. Raeber, G.P., M.P. Lutolf, and J.A. Hubbell, *Molecularly Engineered PEG Hydrogels: A Novel Model System for Proteolytically Mediated Cell Migration.* Biophysical Journal, 2005. **89**(2): p. 1374-1388.
59. Jiang, S., S. Liu, and W. Feng, *PVA hydrogel properties for biomedical application.* Journal of the Mechanical Behavior of Biomedical Materials, 2011. **4**(7): p. 1228-1233.
60. Elliott, J.E., et al., *Structure and swelling of poly(acrylic acid) hydrogels: effect of pH, ionic strength, and dilution on the crosslinked polymer structure.* Polymer, 2004. **45**(5): p. 1503-1510.
61. Dreifus, M., et al., *[Tolerance of orbital implants made of hydrocolloid acrylate]*. Sb Lek, 1960. **62**: p. 212-8.
62. Dreifus, M., O. Wichterle, and D. Lim, *[Intra-cameral lenses made of hydrocolloidal acrylates]*. Cesk Oftalmol, 1960. **16**: p. 154-9.
63. Wichterle, O., D. Lim, and M. Dreifus, *[On the problem of contact lenses]*. Cesk Oftalmol, 1961. **17**: p. 70-5.

64. Kizilel, S., V.H. Perez-Luna, and F. Teymour, *Photopolymerization of poly(ethylene glycol) diacrylate on eosin-functionalized surfaces.* Langmuir, 2004. **20**(20): p. 8652-8.
65. Pierschbacher, M.D. and E. Ruoslahti, *Cell attachment activity of fibronectin can be duplicated by small synthetic fragments of the molecule.* Nature, 1984. **309**(5963): p. 30-33.
66. Pierschbacher, M.D. and E. Ruoslahti, *Variants of the cell recognition site of fibronectin that retain attachment-promoting activity.* Proc Natl Acad Sci U S A, 1984. **81**(19): p. 5985-8.
67. Misra, S.K., et al., *Co-liposomes comprising a lipidated multivalent RGD-peptide and a cationic gemini cholesterol induce selective gene transfection in αvβ3 and αvβ5 integrin receptor-rich cancer cells.* Journal of Materials Chemistry B, 2014. **2**(35): p. 5758.
68. Wickham, T.J., et al., *Integrins alpha v beta 3 and alpha v beta 5 promote adenovirus internalization but not virus attachment.* Cell, 1993. **73**(2): p. 309-19.
69. Nazli, C., et al., *Targeted delivery of doxorubicin into tumor cells via MMP-sensitive PEG hydrogel-coated magnetic iron oxide nanoparticles (MIONPs).* Colloids and Surfaces B: Biointerfaces, 2014. **122**: p. 674-683.
70. Nazli, C., et al., *RGDS-functionalized polyethylene glycol hydrogel-coated magnetic iron oxide nanoparticles enhance specific intracellular uptake by HeLa cells.* Int J Nanomedicine, 2012. **7**: p. 1903-20.
71. Buckley, C.D., et al., *RGD peptides induce apoptosis by direct caspase-3 activation.* Nature, 1999. **397**(6719): p. 534-539.
72. Thalmann, G.N., et al., *Osteopontin: Possible role in prostate cancer progression.* Clinical Cancer Research, 1999. **5**(8): p. 2271-2277.
73. Sugahara, K.N., et al., *Tissue-Penetrating Delivery of Compounds and Nanoparticles into Tumors.* Cancer Cell, 2009. **16**(6): p. 510-520.
74. Weinel, R.J., et al., *THE ALPHA(6)-INTEGRIN RECEPTOR IN PANCREATIC-CARCINOMA.* Gastroenterology, 1995. **108**(2): p. 523-532.
75. Garanger, E., D. Boturyn, and P. Dumy, *Tumor targeting with RGD peptide ligands-design of new molecular conjugates for imaging and therapy of cancers.* Anticancer Agents Med Chem, 2007. **7**(5): p. 552-8.
76. Kibbey, M.C., et al., *A 110-kD nuclear shuttling protein, nucleolin, binds to the neurite-promoting IKVAV site of laminin-1.* J Neurosci Res, 1995. **42**(3): p. 314-22.
77. Chen, X., et al., *Cell surface nucleolin serves as receptor for DNA nanoparticles composed of pegylated polylysine and DNA.* Mol Ther, 2008. **16**(2): p. 333-42.
78. Coopman, P.J., et al., *Integrin alpha 3 beta 1 participates in the phagocytosis of extracellular matrix molecules by human breast cancer cells.* Molecular Biology of the Cell, 1996. **7**(11): p. 1789-1804.

79. Langel, U., et al., *Chimeric constructs between cancer-homing peptides and cell-penetrating peptides coupled to anticancer drugs and/or diagnostic agent/agents*. 2007, Google Patents.
80. Kruse, A.M., et al., *Synthesis and characterization of CREKA-conjugated iron oxide nanoparticles for hyperthermia applications.* Acta Biomaterialia, 2014. **10**(6): p. 2622-2629.
81. Bibette, J., F.L. Calderon, and P. Poulin, *Emulsions: basic principles.* Reports on Progress in Physics, 1999. **62**(6): p. 969.
82. Sobhani, H., et al., *Formulation Development and Toxicity Assessment of Triacetin Mediated Nanoemulsions as Novel Delivery Systems for Rapamycin.* Iranian Journal of Pharmaceutical Research, 2015. **14**: p. 3-21.
83. McAllister, K., et al., *Polymeric Nanogels Produced via Inverse Microemulsion Polymerization as Potential Gene and Antisense Delivery Agents.* Journal of the American Chemical Society, 2002. **124**(51): p. 15198-15207.
84. Peppas, N.A., et al., *Hydrogels in pharmaceutical formulations.* Eur J Pharm Biopharm, 2000. **50**(1): p. 27-46.
85. Bal, T., B. Kepsutlu, and S. Kizilel, *Characterization of protein release from poly(ethylene glycol) hydrogels with crosslink density gradients.* Journal of Biomedical Materials Research Part A, 2014. **102**(2): p. 487-495.
86. Hirata, Y., et al., *Insolubilization of water-soluble dextran.* Biomaterials, 1999. **20**(4): p. 303-307.
87. Porjazoska, A., et al., *Synthesis and characterization of poly(ethylene glycol)-poly(D,L-lactide-co-glycolide) poly(ethylene glycol) tri-block co-polymers modified with collagen: a model surface suitable for cell interaction.* J Biomater Sci Polym Ed, 2006. **17**(3): p. 323-40.
88. Li, H. and J.J. Cooper-White, *Changing ligand number and type within nanocylindrical domains through kinetically constrained self-assembly – impacts of ligand 'redundancy' on human mesenchymal stem cell adhesion and morphology.* Biomater. Sci., 2014. **2**(11): p. 1693-1705.
89. Wen, A.M., et al., *Shaping bio-inspired nanotechnologies to target thrombosis for dual optical-magnetic resonance imaging.* Journal of Materials Chemistry B, 2015. **3**(29): p. 6037-6045.
90. Goncalves, M., et al., *pH-sensitive Laponite((R))/doxorubicin/alginate nanohybrids with improved anticancer efficacy.* Acta Biomater, 2014. **10**(1): p. 300-7.
91. Lewinski, N., V. Colvin, and R. Drezek, *Cytotoxicity of nanoparticles.* Small, 2008. **4**(1): p. 26-49.
92. Kim, T.G. and T.G. Park, *Biomimicking extracellular matrix: cell adhesive RGD peptide modified electrospun poly(D,L-lactic-co-glycolic acid) nanofiber mesh.* Tissue Eng, 2006. **12**(2): p. 221-33.

93. Barczyk, M., S. Carracedo, and D. Gullberg, *Integrins.* Cell and Tissue Research, 2010. **339**(1): p. 269-280.
94. Caniggia, I., et al., *Identification of receptors binding fibronectin and laminin on fetal rat lung cells.* Am J Physiol, 1996. **270**(3 Pt 1): p. L459-68.
95. Furth, J.J., T.H. Wroth, and S. Ackerman, *Genes for collagen types I, IV, and V are transcribed in HeLa cells but a postinitiation block prevents the accumulation of type I mRNA.* Exp Cell Res, 1991. **192**(1): p. 118-21.
96. Angeles, V., et al., *The influence of surface functionalization on the enhanced internalization of magnetic nanoparticles in cancer cells.* Nanotechnology, 2009. **20**(11): p. 115103.
97. Ma, L.L., et al., *Small Multifunctional Nanoclusters (Nanoroses) for Targeted Cellular Imaging and Therapy.* ACS Nano, 2009. **3**(9): p. 2686-2696.
98. Agarwal, A., et al., *Dextran conjugated dendritic nanoconstructs as potential vectors for anti-cancer agent.* Biomaterials, 2009. **30**(21): p. 3588-3596.
99. Furth, J.J., T.H. Wroth, and S. Ackerman, *Genes for collagen types I, IV, and V are transcribed in Hela cells but a postinitiation block prevents the accumulation of type I mRNA.* Experimental Cell Research, 1991. **192**(1): p. 118-121.

VITA

Aysu Ceren Okur was born in Ankara, 1990. She went to high school at Kabataş Erkek Lisesi between 2004- 2008. She completed her undergraduate degree on Materials Science & Engineering & Chemistry at Sabancı University between 2008 and 2013. In 2013, she started Master Degree program on Biomedical Sciences & Engineering at Koc University.